



# UNIVERSITÀ DI PARMA

## ARCHIVIO DELLA RICERCA

University of Parma Research Repository

Inhibition of Eph/ephrin interaction with the small molecule UniPR500 improves glucose tolerance in healthy and insulin-resistant mice

This is the peer reviewed version of the following article:

*Original*

Inhibition of Eph/ephrin interaction with the small molecule UniPR500 improves glucose tolerance in healthy and insulin-resistant mice / Giorgio, C; Incerti, M; Pala, D; Russo, S; Chiodelli, P; Rusnati, M; Cantoni, Am; Di Lecce, R; Barocelli, E; Bertoni, S; Ravassard, P; Manenti, F; Piemonti, L; Ferlenghi, F; Lodola, A; Tognolini, M.. - In: PHARMACOLOGICAL RESEARCH. - ISSN 1096-1186. - 141:(2019), pp. 319-330. [10.1016/j.phrs.2019.01.011]

*Availability:*

This version is available at: 11381/2854571 since: 2021-10-11T16:24:37Z

*Publisher:*

Academic Press

*Published*

DOI:10.1016/j.phrs.2019.01.011

*Terms of use:*

Anyone can freely access the full text of works made available as "Open Access". Works made available

*Publisher copyright*

note finali coverpage

(Article begins on next page)

## Manuscript Details

**Manuscript number** YPHRS\_2018\_812\_R1

**Title** Inhibition of Eph/ephrin interaction with the small molecule UniPR500 improves glucose tolerance in healthy and insulin-resistant mice

**Article type** Research Paper

### Abstract

Eph/ephrin interactions and their bidirectional signaling are integral part of the complex communication system between  $\beta$ -cells, essential for glucose homeostasis. Indeed, Eph/ephrin system was shown to be directly involved in the glucose-stimulated insulin secretion (GSIS) process occurring in the pancreatic islets. Here we tested the Eph antagonist UniPR500 as GSIS enhancer. UniPR500 was validated as EphA5-ephrin-A5 inhibitor in vitro and its efficacy as GSIS enhancer was assessed on EndoC- $\beta$ H1 cells. The selectivity of UniPR500 was evaluated by testing this compound on a panel of well-known molecular targets responsible for the regulation of glucose homeostasis. Plasmatic levels of UniPR500 were measured by HPLC/MS approach after oral administration. Finally, UniPR500 was tested as hypoglycemic agent in healthy mice, in a non-genetic mouse model of insulin resistance (IR) and in a non-genetic mouse model of type 1 diabetes (T1D). The compound is an orally bioavailable and selective Eph antagonist, able to increase GSIS from EndoC- $\beta$ H1 cells. When tested in vivo UniPR500 showed to improve glucose tolerance in healthy and IR mice. As expected by a GSIS enhancer acting on healthy  $\beta$ -cells, UniPR500 was ineffective when tested on a non-genetic mouse model of type 1 diabetes, where pancreatic function was severely compromised. In conclusion our findings suggest that Eph targeting is a new and valuable pharmacological strategy in the search of new hypoglycemic agents.

**Keywords** Eph/ephrin; PPI-inhibitors; protein-protein; diabetes; insulin

**Corresponding Author** Massimiliano Tognolini

**Corresponding Author's Institution** University of Parma

**Order of Authors** Carmine Giorgio, Matteo Incerti, Daniele Pala, Simonetta Russo, Paola Chiodelli, marco rusnati, Anna Maria Cantoni, Rosanna Di Lecce, Elisabetta Barocelli, Simona Bertoni, Philippe Ravassard, Fabio Manenti, Lorenzo piemonti, Francesca Ferlenghi, Alessio Lodola, Massimiliano Tognolini

**Suggested reviewers** Raphael Lamprecht, David Alfaro, Francesca De Franco

## Submission Files Included in this PDF

### File Name [File Type]

Cover letter 2.docx [Cover Letter]

response to referee.docx [Response to Reviewers]

graphical abstract.pptx [Graphical Abstract]

paper diabete 31 cleaned.docx [Manuscript File]

Fig1 129 A5A5.tif [Figure]

Fig2 TGR5.tif [Figure]

Fig3 binding 500.tif [Figure]

Fig4 SPR 500 su A5.tiff [Figure]

Fig5 selectivity.tif [Figure]

Fig6 perfusion.tif [Figure]

Fig7 pk.tif [Figure]

Fig8 IGTT insulina sani.tif [Figure]

Flg9 Model.tif [Figure]

Fig10 basali dopo HFD +500.tif [Figure]

Fig11 IGTT HFD.tif [Figure]

Fig12 IGTT e AUC.tif [Figure]

SUppl material revised.docx [Table]

Table 1 off targets.docx [Table]

Table 2.docx [Table]

COI.docx [Conflict of Interest]

To view all the submission files, including those not included in the PDF, click on the manuscript title on your EVISE Homepage, then click 'Download zip file'.

## Research Data Related to this Submission

There are no linked research data sets for this submission. The following reason is given:  
Data will be made available on request



**UNIVERSITÀ  
DI PARMA**

**DIPARTIMENTO DI SCIENZE  
DEGLI ALIMENTI E DEL FARMACO**

Dear Editor,

please consider the submission of the paper entitled “**Inhibition of Eph-ephrin interaction with the small molecule UniPR500 improves glucose tolerance in healthy and insulin-resistant mice**” by Giorgio C. et al., that we are submitting for publication in *Pharmacological research* on behalf of all authors.

Our research group is engaged from 10 years in the discovery and development of PPI-inhibitors targeting the Eph/ephrin system. These proteins are well known for their primary role during embryogenesis where they regulate cell segregation and tissue differentiation. These proteins are upregulated in the tumor environment where they regulate angiogenesis, the replication of tumor propagating cells and the invasiveness of the cancer. Their expression in the healthy adult is almost missing but recent evidence showed their expression in the pancreas where they regulate Glucose Stimulated Insulin Secretion (Konstantinova et al., 2007). A proof-of-concept about the druggability of the system was offered by Jain et al (2013) by means of kinase inhibitors. In the present paper we showed for the first time that the inhibition of Eph/ephrin interaction by using a small molecule can increase insulin release *in vitro* and in healthy and insulin-resistant mice *in vivo*, resulting in a better glucose tolerance.

This manuscript has been read and approved by all the authors. The criteria for authorship have been met. The manuscript or part of it has neither been published nor is currently under consideration for publication by any other journal. M. Tognolini, A. Lodola and M. Incerti patented the described compound (Italian patent 0001426534, no extensions).

Hoping that our manuscript will be eligible for publication, we convey our best regards.

Sincerely,

*Massimiliano Tognolini*

**UNIVERSITÀ DI PARMA**

Parco Area delle Scienze, 27/A - 43124 Parma

[www.unipr.it](http://www.unipr.it)

**Comments from the editors and reviewers:**

**-Reviewer 1**

-

This paper by C. Giorgio et al. entitled “Inhibition of Eph/ephrin interaction with a small molecule UniPR500 improves glucose tolerance in healthy and insulin-resistant mice” dealt the generation of a novel Eph antagonist UniPR500 more selective for the Eph/ephrin system and featured by a fair oral bio-availability, the authors tested the Eph antagonist UniPR500 as GSIS enhancer. The study is well done; it can be considering for publication after addressing some concerns.

- The figure 3 should be put or as figure 2, or put the actual figure 2 before the figure 3.

This section was re-arranged following the suggests of both the referees. Figure 2 was removed and included in suppl material.

- In the figure 3 should be put the p value.

Done

- In the figure 11 C should be changed the label on y axis.

Done, thank you

- The authors should add the glucagon level in the data showed.

Sorry, we do not have residual plasma to accomplish the request

- This reference should be added:

The novel therapeutic effect of phosphoinositide 3-kinase- $\gamma$  inhibitor AS605240 in autoimmune diabetes. Azzi J et al. Diabetes. 2012 Jun;61(6):1509-18.

Included in the discussion

**-Reviewer 2**

-

In this manuscript, the authors show that targeting Eph-epherin axis with UniPR500 induced a substantial improvement of GSIS in vitro as when applied to a human beta cell line EndoC-BH1 enhanced insulin secretion 5 fold upon glucose stimulation. When tested in vivo, in an insulin resistant model particularly showed a slight improvement og glucose intolerance when compared to HFD-mice mainly at 60 and 120 min after glucose

stimulation. While the use of UniPR500 was ineffective in a streptozotocin treated model, as STZ-treated mice showed a severe glucose intolerance similar to HFD-mice.

Overall, the concepts in this manuscript are interesting, the general design of experiments appropriate, and a tremendous amount of work was carried out. However, there are many details particularly the first part describing/dealing with the design of the inhibitor UniPER500 should be cut to the half and summarized, some if not most the figures should be recalled in supplemental. Authors are also requested to add a sub-heading to every part as their results should be summarized in 3 main sections:

- 1-design of the inhibitor
- 2- effect of targeting Eph-ephrin in vitro
- 3- effect of targeting Eph-ephrin in vivo

Done

The manuscript is lacking an important section, discussion ,where the authors should compared their main findings to authors, authors are required to add this section to the manuscript.

An improved section of discussion was included

One comment regarding the supplemental section:

Showing the histological micrographs of only STZ-HFD mice only while lacking the micrographs related to other studied groups is no longer informative as the authors are required to show one representative micrograph from every studied group.

Pictures included as requested

Lastly it would be informative if the authors could validate their finding through the use of a KO mouse model may be EphA5<sup>-/-</sup> mouse?

We thank the reviewer to give us the opportunity to discuss this point.

Genetic manipulation was used by Konstantinova et al (2007) to assess for the first time the involvement of EphA5 and ephrin-A5 in glucose homeostasis. The employment of Ephrin-A5<sup>-/-</sup> mice demonstrated that ephrin-A5 activation induced insulin release since the lack of this protein resulted in poor or no insulin release upon glucose stimulation. Ephrin-A5<sup>-/-</sup> mice showed a lower glucose tolerance as well.

A dominant negative EphA5 protein (DN-EphA5) lacking its cytoplasmic domain was expressed in MIN6 cells, by Konstantinova as well. DN-EphA5 increased basal and glucose-stimulated insulin secretion, whereas WT EphA5 overexpression decreased

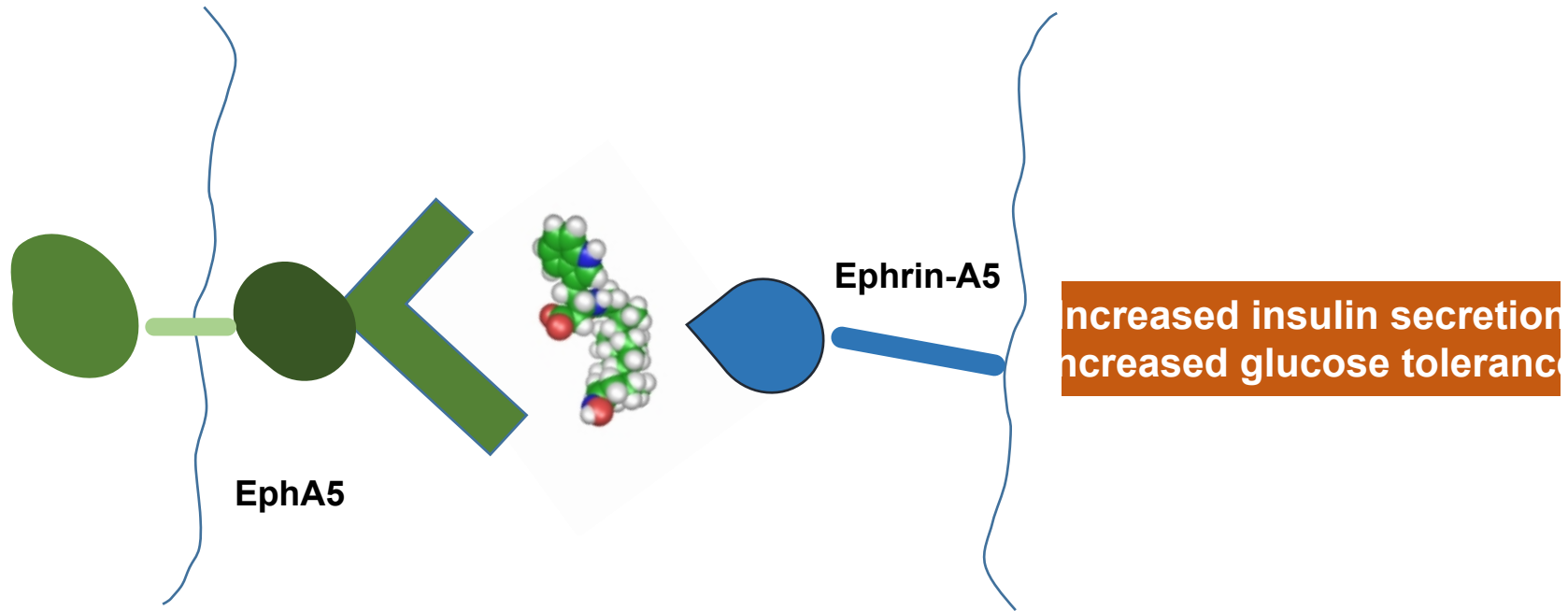
glucose stimulated insulin secretion in confluent MIN6 cells, supporting the idea that EphA forward signaling suppressed insulin secretion.

Ephrin-A5 KO mice were used also by Jain et al (2013) to validate the activity of some kinase inhibitors acting on the EphA5 receptor by measuring insulin levels before and after glucose administration. Ephrin-A5 mice showed an impaired insulin release accordingly to Konstantinova. The administration of the kinase inhibitor did not modify insulin release on ephrin-A5  $-/-$  mice demonstrating that pharmacological inhibition of EphA5 is worthless without ephrin-A5.

EphA5 $-/-$  mice were never studied in this field however, since their behavior can not be related to the effect of DN-EphA5. In fact, you should consider that DN-EphA5 is unable to transduce forward signaling (since it lacks the intracellular domain) but it can activate ephrin-A5 through its extracellular domain and thus increase insulin secretion.

On the other hand EphA5  $-/-$  will be unable to stimulate forward signaling, in accordance with DN-EphA5 but the lack of EphA5 will be unable to stimulate reverse signaling as well, and thus unable to stimulate insulin secretion. In conclusion the use of EphA5  $-/-$  mice can give ambiguous results.

Finally, we tried to validate the activity of our compound not only by characterizing its activity on the Eph receptors but also checking its activity on other systems involved in glucose homeostasis such as TGR5, GLP1, PPAR- $\gamma$ , PTP1B, DPP IV and  $K_{ATP}$  channel, where it showed no activity.



1  
2  
3 **Inhibition of Eph/ephrin interaction with the small molecule UniPR500 improves**  
4 **glucose tolerance in healthy and insulin-resistant mice**  
5  
6  
7

8 **Running title: Eph antagonists and diabetes**  
9

10 C. Giorgio,<sup>1</sup> M. Incerti,<sup>1</sup> D. Pala,<sup>1#</sup> S. Russo,<sup>1</sup> P. Chiodelli,<sup>2</sup> M. Rusnati,<sup>2</sup> A. M. Cantoni,<sup>3</sup> R. Di Lecce,<sup>3</sup> E.  
11 Barocelli,<sup>1</sup> S. Bertoni,<sup>1</sup> P. Ravassard,<sup>4</sup> F. Manenti,<sup>5</sup> L. Piemonti,<sup>5,6</sup> F. Ferlenghi,<sup>1</sup> A. Lodola,<sup>1</sup> M. Tognolini,<sup>1</sup>  
12  
13  
14

15  
16 <sup>1</sup>*Dipartimento di Scienze degli Alimenti e del Farmaco, Università degli Studi di Parma, Parma, Italy.*  
17

18  
19 <sup>2</sup>*Dipartimento di Medicina Molecolare Traslazionale, Università degli Studi di Brescia, Brescia, Italy.*  
20

21  
22 <sup>3</sup>*Dipartimento di Scienze Medico-Veterinarie, Università degli Studi di Parma, Parma, Italy.*  
23

24  
25 <sup>4</sup>*Université Pierre et Marie Curie-Paris 6, Biotechnology and Biotherapy Team, Centre de Recherche de*  
26 *l'Institut du Cerveau et de la Moelle épinière (CRICM), UMRS 975, Paris, France.*  
27  
28

29  
30 <sup>5</sup>*Diabetes Research Institute, IRCCS San Raffaele Scientific Institute, Milano, Italy.*  
31

32  
33 <sup>6</sup>*Università Vita-Salute San Raffaele, Milano, Italy.*  
34

35 # Actual Address: Chemistry Research and Drug Design Department, Chiesi Farmaceutici S.p.A. , Largo  
36 F. Belloli 11/A, 43122 Parma, Italy.  
37  
38

39  
40 **AUTHOR INFORMATION**

41 **Corresponding Author**

42 Prof. Massimiliano Tognolini

43 Dipartimento di Scienze degli Alimenti e del Farmaco, Università degli Studi di Parma

44 Viale delle Scienze 27/A, 43124 Parma, Italy

45 Phone: +39 0521 906021

46 Fax: +39 0521 906021

47 E-mail: [massimiliano.tognolini@unipr.it](mailto:massimiliano.tognolini@unipr.it)  
48  
49  
50  
51  
52  
53

57  
58  
59 **ABSTRACT**  
60

61 Eph/ephrin interactions and their bidirectional signaling are integral part of the complex communication system  
62 between  $\beta$ -cells, essential for glucose homeostasis. Indeed, Eph/ephrin system was shown to be directly involved  
63 in the glucose-stimulated insulin secretion (GSIS) process occurring in the pancreatic islets. Here we tested the  
64 Eph antagonist UniPR500 as GSIS enhancer.  
65  
66  
67

68 UniPR500 was validated as EphA5-ephrin-A5 inhibitor *in vitro* and its efficacy as GSIS enhancer was assessed on  
69 *EndoC- $\beta$ H1* cells. The selectivity of UniPR500 was evaluated by testing this compound on a panel of well-known  
70 molecular targets responsible for the regulation of glucose homeostasis. Plasmatic levels of UniPR500 were  
71 measured by HPLC/MS approach after oral administration. Finally, UniPR500 was tested as hypoglycemic agent  
72 in healthy mice, in a non-genetic mouse model of insulin resistance (IR) and in a non-genetic mouse model of  
73 type 1 diabetes (T1D).  
74  
75  
76  
77

78 The compound is an orally bioavailable and selective Eph antagonist, able to increase GSIS from *EndoC- $\beta$ H1* cells.  
79 When tested *in vivo* UniPR500 showed to improve glucose tolerance in healthy and IR mice. As expected by a  
80 GSIS enhancer acting on healthy  $\beta$ -cells, UniPR500 was ineffective when tested on a non-genetic mouse model  
81 of type 1 diabetes, where pancreatic function was severely compromised.  
82  
83  
84

85 In conclusion our findings suggest that Eph targeting is a new and valuable pharmacological strategy in the search  
86 of new hypoglycemic agents.  
87  
88  
89  
90  
91  
92  
93  
94  
95  
96  
97  
98  
99  
100  
101  
102  
103  
104  
105  
106  
107  
108  
109  
110  
111  
112

113  
114  
115 **INTRODUCTION**  
116

117 Over the last three decades, several studies concurred to demonstrate that the communication between  $\beta$  cells  
118 contributes to glucose homeostasis by inhibiting insulin secretion from pancreatic islets during fasting while  
119 enhancing it after food intake [1]. In 2007, Konstantinova and collaborators revealed that Eph/ephrin system  
120 participated to the  $\beta$  cells communication network and was directly involved in the glucose-stimulated insulin  
121 secretion (GSIS) process occurring in the pancreatic islets [2].  
122  
123  
124

125 The Eph receptors (erythropoietin-producing hepatocellular carcinoma) represent the largest family of receptor  
126 tyrosine kinases (RTK) in humans. They are divided in 2 classes, EphA and EphB, based on sequence homology of  
127 extracellular domain and their affinity for ephrin ligands, proteins tethered to the cell membrane by either  
128 glycosylphosphatidyl-inositol (GPI) linkage (ephrin-As) or a transmembrane domain in turn linked to a  
129 cytoplasmic tail (ephrin-Bs)[3]. The unique characteristic of these RTK is that upon Eph/ephrin interaction a  
130 bidirectional signaling is generated: in fact not only the Eph receptors (“forward signaling”), but also the ephrins  
131 (“reverse signaling”) are able to transduce signals into the cells [4]. EphA receptors and ephrin-A ligands are  
132 expressed in human and rodent pancreas [5] and pancreatic  $\beta$  cells use EphA/ephrin-A bidirectional signaling to  
133 modulate insulin secretion [2]. In particular, EphAs forward signals work as a brake for insulin release whilst  
134 ephrin-As reverse signals stimulate it. When mice are in a condition of satiety, EphAs forward signals are in part  
135 attenuated by phosphatases activated by glucose and consequently this cellular communication system is  
136 unbalanced toward ephrin-As reverse signals that prompt insulin secretion in the blood stream. Among all the  
137 cloned Eph receptors and ephrin proteins, EphA5 and its cognate ligand ephrin-A5, co-expressed in  $\beta$  cells, are  
138 critical for this process [6].  
139  
140  
141  
142  
143  
144  
145  
146  
147

148 The involvement of the Eph/ephrin system and in particular of EphA5 receptor in the GSIS process has been  
149 unequivocally demonstrated through its pharmacological inhibition by means of RTK inhibitors featured by a 4-  
150 methyl-N-(3-(trifluoromethyl)phenyl)benzamide core, also present in the clinically approved bcr-abl inhibitor  
151 Nilotinib. Intraperitoneal administration of these benzamide derivatives enhanced glucose stimulated insulin  
152 secretion from mouse and human pancreatic islets *in vitro* and increased plasma insulin and glucose tolerance  
153 *in vivo*. At the same time they did not affect glucose homeostasis in *Efna5*<sup>-/-</sup> mice providing the proof-of-concept  
154 that the modulation of the Eph/ephrin system represents a new strategy for the treatment of T2D.  
155  
156  
157  
158

159 An alternative way to inhibit the signaling transduced by the Eph/ephrin system is through the use of compounds  
160 able to bind their extracellular ligand binding domain and thus to prevent their associations to the ephrin-A  
161 ligands [7]. Among the classes of available small molecules targeting the Eph receptors, amino-acid conjugates  
162 of bile acids are emerging as promising agents, as they possess good potency towards Eph receptors in binding  
163  
164  
165  
166  
167  
168

169  
170  
171 and functional assays [8–11]. These compounds possess two key advantages over traditional RTK inhibitors: *i*  
172 they can block the activity of the Eph receptors without having to enter into the cells, *ii* they have the potential  
173 to be more selective than agents designed to mimic the structure of the ubiquitous ATP molecule. The most  
174 potent small-molecule antagonist direct to the extracellular domain of the Eph receptors is UniPR129, L-  $\beta$ -  
175 homotryptophan conjugate of lithocholic acid (LCA) [8]. While UniPR129 exhibited submicromolar inhibitory  
176 activity on Eph receptors, its *in vivo* use has been so far hampered by low bio-availability and off-target activity,  
177 which also includes proteins involved in the regulation of the glucose homeostasis, such as the well-known TGR5  
178 receptor.  
179  
180  
181  
182  
183

184 In the present work, starting from the structure of UniPR129 we provide evidence that following a structure-  
185 based drug design approach it is possible to generate a novel Eph antagonist more selective for the Eph/ephrin  
186 system and featured by a fair oral bio-availability. Thanks to this novel pharmacological tool, we will show that  
187 the antagonism at the extracellular domain of the EphA receptors is a viable strategy to control glucose levels in  
188 normal and obese mice. Our findings not only confirm the involvement of the Eph/ephrin system in glucose and  
189 insulin homeostasis but propose Eph antagonists as potential antidiabetic agents.  
190  
191  
192  
193

## 194 **METHODS**

### 195 **ELISA assays and $K_i$ /IC<sub>50</sub> determination**

196 ELISA assays were performed as previously described [8]. Briefly, 96-well ELISA high binding plates (Costar,  
197 Corning, New York, NY, USA #9018) were incubated overnight at 4 °C with 100 $\mu$ L/well of 1  $\mu$ g mL<sup>-1</sup> EphA5-Fc  
198 (R&D systems, Minneapolis, MN, USA, #541-A5) diluted in sterile phosphate buffered saline (PBS, 0.2 g L<sup>-1</sup> KCl,  
199 8.0 g L<sup>-1</sup> NaCl, 0.2 g L<sup>-1</sup> KH<sub>2</sub>PO<sub>4</sub>, 1.15 g L<sup>-1</sup> Na<sub>2</sub>HPO<sub>4</sub>, pH 7.4). The day after wells were washed with washing buffer  
200 (PBS +0.05% tween20, pH 7.4) and blocked with blocking solution (PBS + 0.5% BSA) for 1 hour at 37 °C.  
201 Compounds were added to the wells at proper concentrations in 1% DMSO and incubated at 37 °C for 1 hour.  
202 Biotinylated ephrin-A5-Fc (R&D systems, Minneapolis, MN, USA, #BT374) was added at 37 °C for 4 hours at its  $K_D$   
203 in displacement assays or in a range from 1 to 2000 ng mL<sup>-1</sup> in saturation studies. Then wells were washed and  
204 incubated with 100 $\mu$ L/well Streptavidin-HRP (Sigma-Aldrich, Milan, Italy, #S5512) for 20 minutes at room  
205 temperature, washed again and finally incubated at room temperature with 0.1 mg mL<sup>-1</sup> tetra-methylbenzidine  
206 (Sigma-Aldrich, Milan, Italy, #860336) reconstituted in stable peroxide buffer (11.3 g L<sup>-1</sup> citric acid, 9.7 g L<sup>-1</sup> sodium  
207 phosphate, pH 5.0) and 0.02% H<sub>2</sub>O<sub>2</sub> (30% m/m in water), added immediately before use. The reaction was  
208 stopped with 3N HCl 100  $\mu$ L/well and the absorbance was measured using an ELISA plate reader (Sunrise, TECAN,  
209 Switzerland) at 450 nm. IC<sub>50</sub> values were determined using one-site competition non-linear regression analysis  
210 with Prism software (GraphPad Software Inc., La Jolla, CA, USA). To assess the selectivity of compounds, all EphA  
211  
212  
213  
214  
215  
216  
217  
218  
219  
220  
221  
222  
223  
224

225  
226  
227 (R&D systems, Minneapolis, MN, USA, #SMPK1) and EphB (R&D systems, Minneapolis, MN, USA, #SMPK2)  
228  
229 receptors were incubated overnight similarly to EphA5-Fc as previously described; biotinylated ephrin-A1-Fc or  
230  
231 biotinylated ephrin-B1-Fc (R&D systems, Minneapolis, MN, USA, #BT602 and #BT473, respectively) at their  $K_D$   
232  
233 were used towards EphAs or EphBs, respectively.  
234

### 235 **Surface plasmon resonance**

236  
237 Surface plasmon resonance (SPR) measurements were performed on a BIAcore X100 instrument (GE-Healthcare,  
238  
239 Milwaukee, WI, USA), using research-grade CM4 carboxyl-methyl-dextran-coated sensorchips (GE-Healthcare,  
240  
241 Milwaukee, WI, USA). SPR was exploited to measure changes in refractive index caused by the binding of  
242  
243 UniPR500 to surface-immobilized EphA5 receptor. To this aim, the fusion protein EphA5-Fc (R&D systems,  
244  
245 Minneapolis, MN, USA, #541-A5) or the Fc fragment alone (Merck Millipore, Darmstadt, Germany, #AG714) were  
246  
247 dissolved at 20  $\mu\text{g}/\text{mL}$  in 10 mM sodium acetate pH 4.0 and allowed to react with two separate flow cells of a  
248  
249 CM4 sensorchip, pre-activated with 50 mL 0.2 M N-ethyl-N-(3-diethylaminopropyl) carbodiimide hydrochloride  
250  
251 and 0.05 M N-hydroxysuccinimide, leading to the immobilization of 3000 and 950 RU for EphA5-Fc and Fc  
252  
253 fragment, respectively. Increasing concentrations of UniPR500 in PBS, 0.05% surfactant P20 and 5% DMSO, pH  
254  
255 7.4 were injected over the EphA5 or Fc surfaces for 90 seconds and then washed until dissociation was observed.  
256  
257 Binding parameters were calculated by the non-linear curve fitting software package BIA evaluation 3.2 using a  
258  
259 single site model with correction for mass transfer (GE Healthcare Europe GmbH, Milan, Italy). Dissociation  
260  
261 constant ( $K_D$ ) was obtained with a steady state analysis, by fitting the bound RU at equilibrium versus the ligand  
262  
263 concentration in solution with a proper form of the Scatchard equation.  
264  
265  
266  
267  
268  
269  
270

### 260 **UniPR500 Off-targets**

261  
262 Stimulant or inhibitory effects of UniPR500 towards GLP1 receptor and PPAR- $\gamma$  receptor as well as the inhibitory  
263  
264 effect versus protein tyrosine phosphatase 1B (PTP1B), dipeptidyl peptidase IV (DPPIV) and ATP-sensitive  
265  
266 potassium channel ( $K_{ATP}$  channel) were performed at CEREP (Eurofins Cerep SA, Celle L'Evescault, France). Test  
267  
268 codes are reported in Table 1. The activity of UniPR500 towards TGR5 receptor was performed at INTERCEPT  
269  
270 (Intercept, London, UK).

### 271 **EndoC- $\beta$ H1**

272  
273 The genetically engineered human pancreatic  $\beta$  cell line EndoC- $\beta$ H1, kindly provided us by Professor Ravassard  
274  
275 [12], was grown in DMEM low glucose (1 g/L) (ThermoFisher Scientific, Waltham, MA, USA, #11885084), 2% BSA,  
276  
277 50  $\mu\text{M}$  2-mercaptoethanol (Sigma-Aldrich, Milan, Italy, #M3148), 10 mM nicotinamide (Sigma-Aldrich, Milan,  
278  
279  
280

Italy, #N0636), 5.5 µg/mL transferrin (ThermoFisher Scientific, Waltham, MA, USA, #11107018), 6.7 ng/mL sodium selenite (Sigma-Aldrich, Milan, Italy, #S5261), 1% Pen/Strep.

### **Dynamic perfusion**

A high-capacity, automated perfusion system (Bio rep® Perifusion V2.0.0) was used to dynamically measure insulin secretion from EndoC-βH1 cells. A low pulsatility peristaltic pump pushed HEPES-buffered solution (125 mM NaCl, 5.9 mM KCl, 2.56 mM CaCl<sub>2</sub>, 1 mM MgCl<sub>2</sub>, 25 mM HEPES, 0.1% BSA, pH 7.4) through a sample container harboring 7\*10<sup>5</sup> EndoC-βH1 cells. Cells were stabilized in the machine with a 200µl/min flow perfusion rate with low glucose (2mM) for 60 minutes. Combination of stimuli (2 and 20 mM Glucose, 10 µM UniPr500 and 0.1% DMSO as vehicle) were then added for 20 minutes at a flow rate of 200 µl/min, followed by another 20 minutes with low glucose (2 mM) to evaluate ability of cells to recover the basal insulin secretion. The perfusates were collected every minute in an automatic fraction collector designed for multiwell plate format. Cells and the perfusion solutions were kept at 37°C in a built-in temperature controlled chamber, and the perfusate in the collecting plate was kept at <15°C.

### **Animals.**

All animal experiments were authorized by the local Animal Care Committee and by the Italian Ministry of Health. All procedures involving animals and their care were performed according to the Italian (DL 26/2014) and European (Directive 2010/63/EU) laws and policies on the protection of animals used for scientific purposes.

### **Non-genetic mouse model of Insulin-Resistance**

C57BL/6J mice were fed *ad libitum* for 10 weeks with high-fat diet (HFD, 60% calories from fat, Mucedola, Milan, Italy) in order to induce insulin resistance and, as a consequence, impaired glucose tolerance [13]. After eight weeks of high fat diet, animals with an insulin level higher than 1.20ng/dl and plasma glucose higher than 190mg/dl, were randomly divided in two groups. UniPR500 (30 mg/kg) or methocel alone were orally administered for the next 14 days, from the 9<sup>th</sup> to the 10<sup>th</sup> week of HFD treatment. The last administration was done 30 minutes before performing glucose tolerance test. C57BL/6J mice fed with standard diet (Mucedola, Milan, Italy) were used as healthy control.

Mice weight, fasting blood glucose and cholesterol levels were evaluated right before the beginning of the pharmacological treatment and the day before the last administration, in order to evaluate the effect of drug on disease progression.

337  
338  
339 **Non-genetic mouse model of Type 1 diabetes**  
340

341 C57BL/6J mice were injected with streptozotocin 40mg/kg i.p. for 5 consecutive days (days 1-5) and fed *ad*  
342 *libitum* for at least 6 weeks (days 6-50) with high-fat diet in order to induce metabolic characteristics of T1D such  
343 as increased fasting blood glucose levels and impaired glucose tolerance [14]. At day 37 mice were randomly  
344 divided in two group. UniPR500 (30 mg/kg) or methocel alone were orally administered for 14 days, from the  
345 day 37 to the day 50 and the last administration was done 30 minutes before performing glucose tolerance test.  
346 C57BL/6J mice fed with standard diet (Mucedola, Milan, Italy) were used as healthy control.  
347  
348  
349

350  
351 **Intraperitoneal glucose tolerance test (IGTT)**  
352

353 Glucose tolerance test was performed on fasted male C57BL/6J mice. Healthy mice, insulin resistant mice (IR)  
354 and diabetic type 1 animals (T1D) were challenged by intraperitoneal injection of 2 g glucose/kg body weight.  
355 Glucose levels were measured in plasma by means of a colorimetric assay (Instrumentation Laboratory Kit,  
356 Karlsruhe, Germany, #0018259140).  
357  
358  
359

360 **Plasma insulin and cholesterol determination**  
361

362 Plasma insulin and cholesterol levels were determined by mean of an insulin ELISA assay (Merck Millipore,  
363 Darmstadt, Germany, #EZRFMI-13K) and a colorimetric assay (Instrumentation Laboratory Kit, Karlsruhe,  
364 Germany, #0018250540), respectively.  
365  
366

367 **Anatomo-pathological analysis**  
368

369 Anatomo-pathological analysis were performed on streptozotocin-HFD mice treated and untreated with  
370 UniPR500 30mg/kg os for 14 days. Liver, kidneys, pancreas were collected from each mice and samples were  
371 immediately fixed in 10% neutral buffered formalin. After paraffin embedding, 4-5  $\mu$ m thick sections, were  
372 obtained with microtome (Leica), stained with Hematoxylin and Eosin (H&E) and Periodic acid-Schiff (PAS).  
373 Histological slides were examined with Nikon Eclipse E800 microscope (Nikon Corporation, Japan) using Nikon  
374 PLAN APO lenses. Sections were photographed at 4x, 10x, 20x and 40x (Nikon PLAN APO lenses) with Camera  
375 DIGITAL SIGHT DS-Fi1 (Nikon Corporation, made in Japan); pictures were acquired with DS Camera Control Unit  
376 DS-L2 (Nikon Corporation, Japan) and stored in USB device. Histological lesions were graded and classified  
377 based on the extension/distribution (focal, multifocal and diffuse) and severity (scant, mild, moderate, severe).  
378  
379  
380  
381  
382

383 **Data and statistical analysis**  
384

385 Results are expressed as mean  $\pm$  SD or percentage  $\pm$  SD change versus controls. Statistical significance was  
386 evaluated by one way-ANOVA or two-way ANOVA followed by Dunnett's or Bonferroni test, respectively. The  
387  
388  
389  
390  
391  
392

393  
394  
395 *post hoc* tests were run only if F achieved  $p < 0.05$  and there was no significant variance inhomogeneity. A  $p$ -  
396 value  $< 0.05$  was considered significant. All statistical tests were performed on raw or normalized data  
397 (perifusion) using the Prism Graph Pad 5.01 (La Jolla, California, USA). Insulin release during perifusion was  
398 normalized to basal value. More details are reported in the legend of the pictures.  
400

## 401 402 **RESULTS**

### 403 404 **Design of the inhibitor**

405  
406 We previously identified UniPR129 as a tool inhibiting EphA2/ephrin-A1 binding *in vitro* [8] and we asked whether  
407 UniPR129 was able to interfere with EphA5/ephrin-A5 binding since they are involved in insulin release. We  
408 immobilized the EphA5-Fc ectodomain on ELISA plates and detected the binding of biotinylated ephrin-A5-Fc.  
409 UniPR129 dose-dependently reduced EphA5/ephrin-A5 interaction with an  $IC_{50}$  value of  $1.2 \mu\text{M}$  (Figure 1A).  
410 Saturation curves of EphA5/ephrin-A5 were built in the presence of increasing UniPR129 concentrations allowing  
411 to calculate  $K_D$  and apparent  $K_D$  values. These values were used to draw a Schild plot [15] (Figure 1B and 1C)  
412 characterized by a well-interpolated regression line ( $r^2=0.98$ ) with a slope of 0.91. The  $pK_i$  resulting from the  
413 intersection of the interpolated line with the X-axis was  $6.11 \pm 0.07$  (corresponding to a  $K_i$  of  $0.77 \mu\text{M}$ ). The  
414 removal of UniPR129 from the displacement assay wells through a washing procedure restores ephrin-A5 binding  
415 to EphA5 (Figure 1D). Taken together, these data suggest a competitive and reversible antagonism of UniPR129  
416 at the EphA5 receptor.  
417  
418  
419  
420  
421  
422  
423  
424  
425  
426  
427  
428  
429  
430  
431  
432  
433  
434  
435  
436  
437  
438  
439  
440  
441  
442  
443  
444  
445  
446  
447  
448

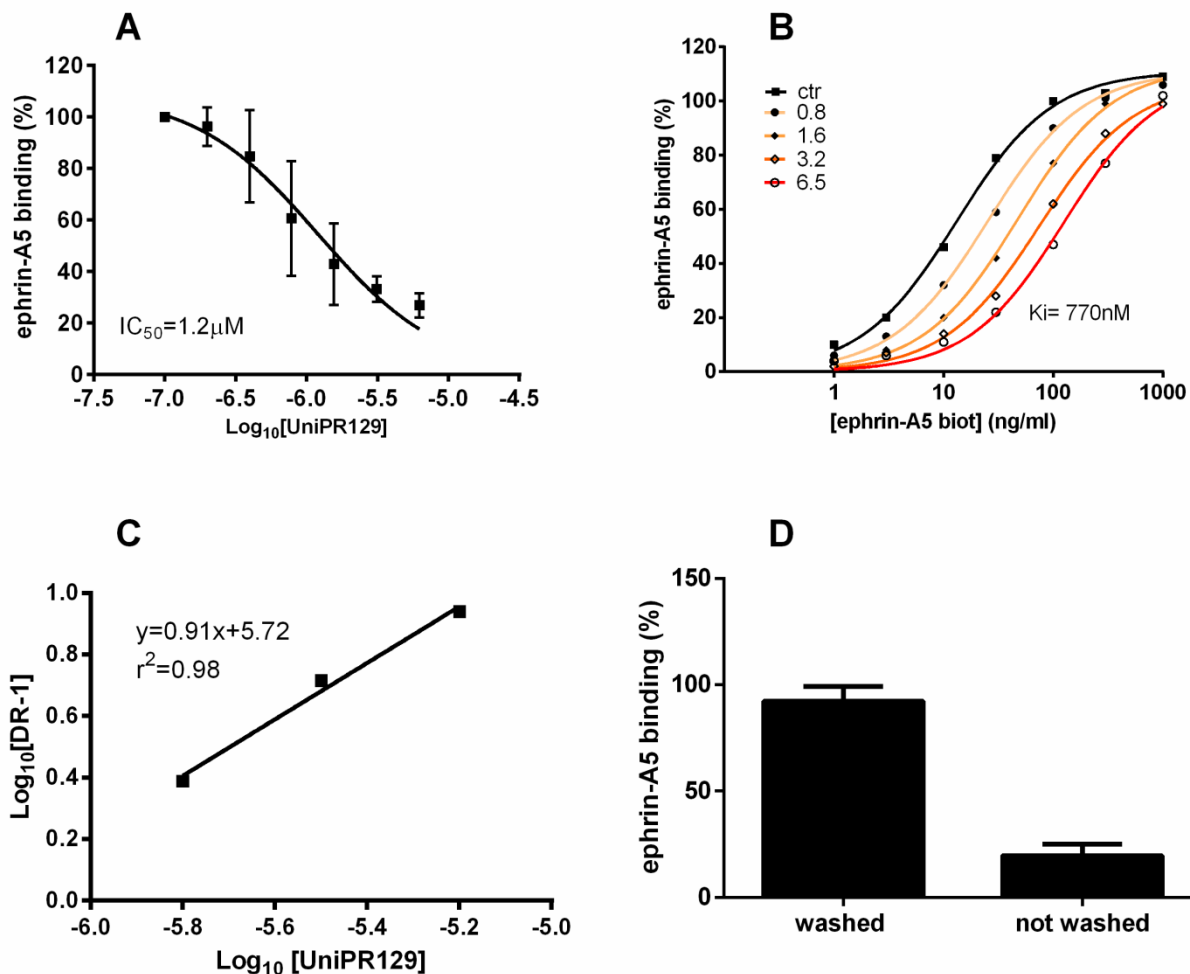


Figure 1 **A**, UniPR129 dose-dependently displaced the binding of biotinylated ephrin-A5-Fc from immobilized EphA5-Fc. **B**, binding of biotinylated ephrin-A5-Fc to immobilized EphA5-Fc ectodomain in the presence of different concentrations of UniPR129. **C**, the dissociation constants ( $K_D$ ) from the previous plot were used to calculate  $\text{Log}_{10}(\text{Dose-ratio} - 1)$  and to graph the Schild plot.  $\text{pK}_i$  of UniPR129 was estimated by the intersection of the interpolated line with the X-axis. **D**, EphA5-ephrin-A5 binding in the presence of 10  $\mu\text{M}$  UniPR129 with or without washing three times with PBS before adding biotinylated ephrin-A5-Fc. Data are the means of at least four independent experiments  $\pm$  st. dev.

Amino acid conjugates of LCA have been reported to activate TGR5, a G-protein coupled receptor responsive to bile acids, in the micromolar range [16]. This is also the case of UniPR129 which activates TGR5 in CHO cells with an  $\text{EC}_{50}$  of 3.9  $\mu\text{M}$  (figure 2). TGR5 agonists, such as the clinical candidate INT-777, have been shown to enhance glucose tolerance in obese mice [17]. Considering our willingness to assess the impact of an Eph antagonist on

505  
506  
507 glucose homeostasis, the availability of a molecule lacking of any activity on TGR5 receptor was a mandatory  
508 step of our research program. To this end, we built a homology model of TGR5 according to procedure reported  
509 by Macchiarulo and colleagues [18] to identify a likely binding mode for UniPR129. Docking simulations,  
510 performed as described in reference [19], identified a top-ranked model where UniPR129 interacted with Ser270  
511 thanks to its carboxylate and with Asn93 by its 3 $\alpha$ -hydroxyl group (Figure S1, left panel, supplementary material).  
512 Starting from this interaction model, we hypothesized that the introduction of a 3 $\alpha$  substituent bulkier than a  
513 hydroxyl group, (i.e. not able any more to bind Asn93) would lead to a compound inactive on TGR5. Docking  
514 simulations confirmed our working hypothesis as in the top-ranked docking pose, the 3-hydroxyimino analogue  
515 UniPR500 failed to undertake polar interactions with the key asparagine Asn93 (Figure S1, right panel). We also  
516 evaluated *in silico* if the same chemical modification was tolerated by the EphA5 receptor. Docking simulations  
517 indicated that UniPR129 and UniPR500 bound EphA5 with the same orientation and that the H-bond undertaken  
518 by the 3 $\alpha$  hydroxyl of UniPR129 with Glu88 could be also undertaken by the corresponding 3-hydroxyimino group  
519 of UniPR500 (Figure S2). This computational investigation suggested that UniPR500 may selectively bind EphA5  
520 receptor.  
521  
522

523  
524 In order to confirm computational data, the 3-hydroxyimino derivative UniPR500 was thus tested for its ability  
525 to activate the TGR5 receptor in comparison with UniPR129 and deoxycolic acid (DCA) in a functional assay  
526 developed by DiscoverX. In this experiment CHO cells were incubated with compounds and cAMP production  
527 was correlated to the activation of TGR5 receptor. As mentioned above and reported in figure 2 UniPR129 dose-  
528 dependently activated TGR5 with a EC<sub>50</sub> of 3.4  $\mu$ M and reached a maximal response of 80 % in comparison with  
529 DCA, used as positive control [20]. Conversely UniPR500 failed to activate TGR5 receptor showing a negligible  
530 response at the highest concentration tested (30  $\mu$ M).  
531  
532  
533  
534  
535  
536  
537  
538  
539  
540  
541  
542  
543  
544  
545  
546  
547  
548  
549  
550  
551  
552  
553  
554  
555  
556  
557  
558  
559  
560

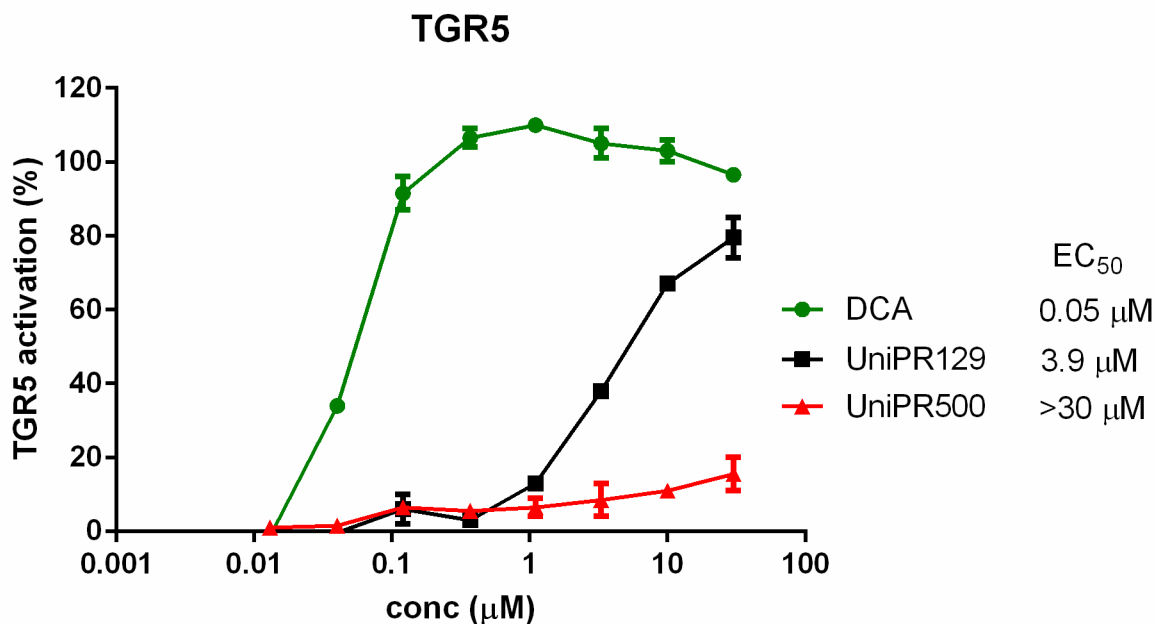


Figure 2. Dose response curve for TGR5 activation in CHO cells. Activation of the receptor was assessed measuring the production of cAMP level. Green line, deoxycholic acid; black line, UniPR129; red line UniPR500. Experiments are performed in duplicate.

UniPR500 was thus tested for its ability to disrupt EphA5-ephrin-A5 interaction by using the ELISA assay described above. The compound was still able to inhibit EphA5-ephrin-A5 interaction with an IC<sub>50</sub> value of 3.7 μM (Figure 3A) comparable to UniPR129, indicating that the EphA5 receptor is significantly more tolerant versus chemical modification than TGR5 receptor.

Saturation curves of EphA5-ephrin-A5 binding in the presence of increasing UniPR500 concentrations allowed us to draw a Schild plot (Figure 3B and 3C). We obtained a well-interpolated regression line ( $r^2=0.92$ ) with a slope of 0.84, consistent with a competitive antagonism. The resulting K<sub>i</sub> was  $1.7\pm 0.2$  μM. The removal of UniPR500 from the binding assay wells through washing, restores ephrin-A5 binding to EphA5 indicating that UniPR500 acts as a reversible antagonist (Figure 3D).

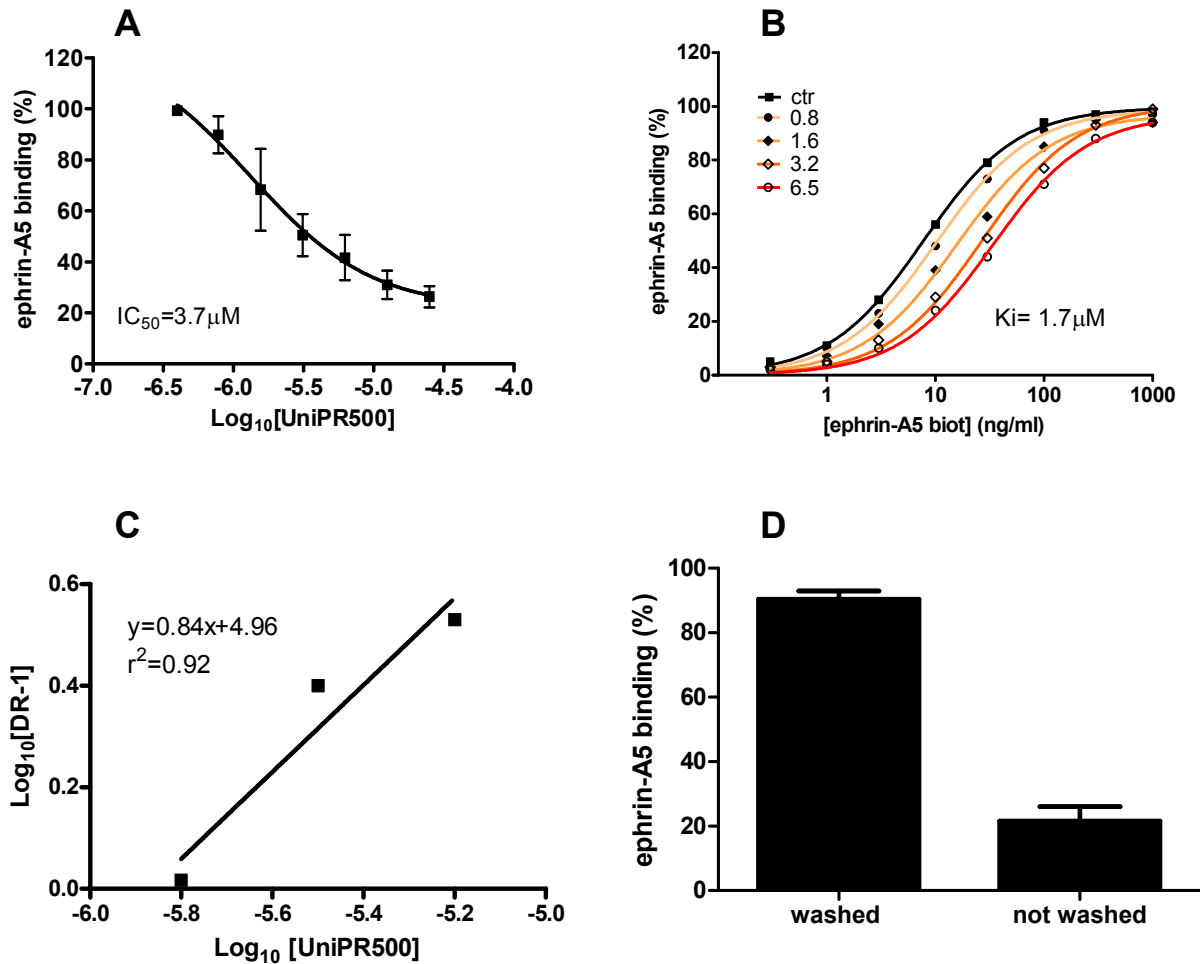
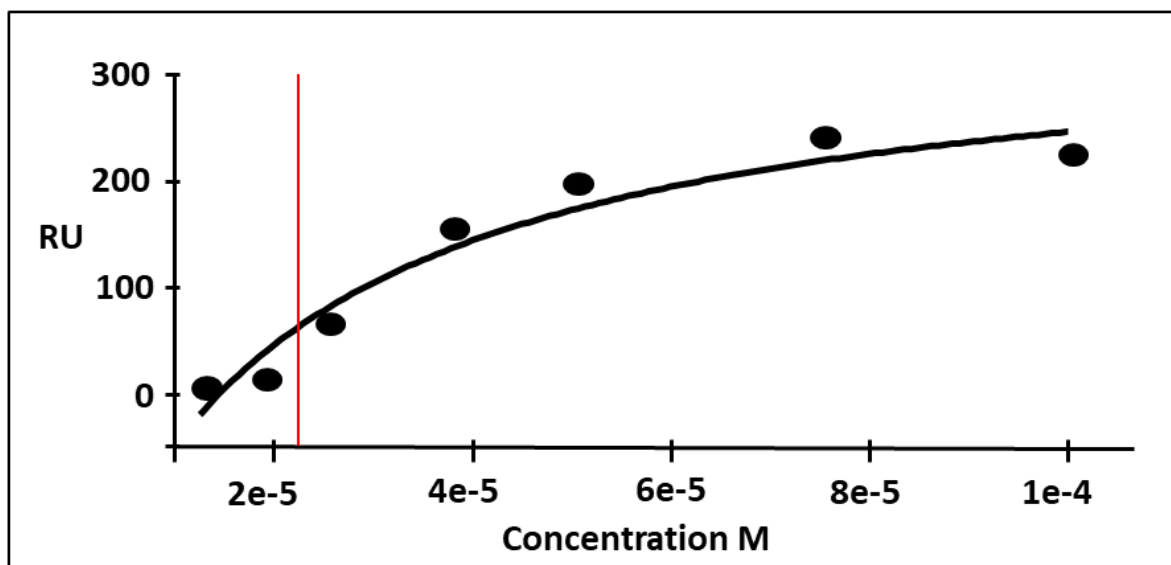


Figure 3 **A**, UniPR500 dose-dependently displaced the binding of biotinylated ephrin-A5-Fc from immobilized EphA5-Fc. **B**, binding of biotinylated ephrin-A5-Fc to immobilized EphA5-Fc ectodomain in the presence of different concentrations of UniPR500. **C**, the dissociation constants ( $K_D$ ) from the previous plot were used to calculate  $\text{Log}_{10}(\text{Dose-ratio} - 1)$  and to graph the Schild plot.  $pK_i$  of UniPR500 was estimated by the intersection of the interpolated line with the X-axis. **D**, EphA5-ephrin-A5 binding in the presence of  $10 \mu M$  UniPR500 with or without washing three times with PBS before adding biotinylated ephrin-A5-Fc. Data are the means of at least four independent experiments  $\pm$  st. dev.

### UniPR500 binds EphA5 receptor

We next set a surface plasmon resonance (SPR) assay to characterize the mechanism of interaction between UniPR500 and EphA5 at a molecular level. UniPR500 binds surface-immobilized EphA5 in a concentration-dependent way with saturation binding reached at concentrations ranging between  $60$  and  $80 \mu M$  (Figure 4).

673  
674  
675 The dissociation constant ( $K_D$ ) measured from steady state analysis results equal to 22  $\mu$ M.  
676  
677



694  
695 *Figure 4. Steady state analysis of the interaction of UniPR500 with EphA5-Fc immobilized to a SPR sensorchip.*  
696 *The saturation curve is obtained by plotting the blank subtracted RU values at equilibrium resulting from the*  
697 *injection of increasing concentrations of UniPR500 onto the Eph5-Fc surface versus the UniPR500 concentration.*  
698 *Black line represents the fitted curve while the redline identifies the  $K_D$  value, as equal to the concentration*  
699 *yielding 50% of the maximum response.*  
700  
701

#### 702 703 704 705 **UniPR500 is a pan Eph/ephrin inhibitor**

706  
707 The selectivity of UniPR500 interaction versus the different EphA and EphB receptors was studied using  
708 biotinylated ephrin-A1-Fc and biotinylated ephrin-B1-Fc, respectively, at their  $K_D$  concentrations. As showed in  
709 Figure 5 the compound inhibited the interaction of ephrin-A1-Fc or ephrin-B1-Fc with all Eph receptors. The  $IC_{50}$   
710 values for EphA receptors ranged from 1.14 to 1.52  $\mu$ M whilst for EphB receptors were in the 2.05-5.09  $\mu$ M range  
711 (Figure 5). UniPR500 can thus be regarded as a pan-antagonist of the Eph receptors targeting their highly  
712 conserved ligand binding domain [19].  
713  
714  
715  
716  
717  
718  
719  
720  
721  
722  
723  
724  
725  
726  
727  
728

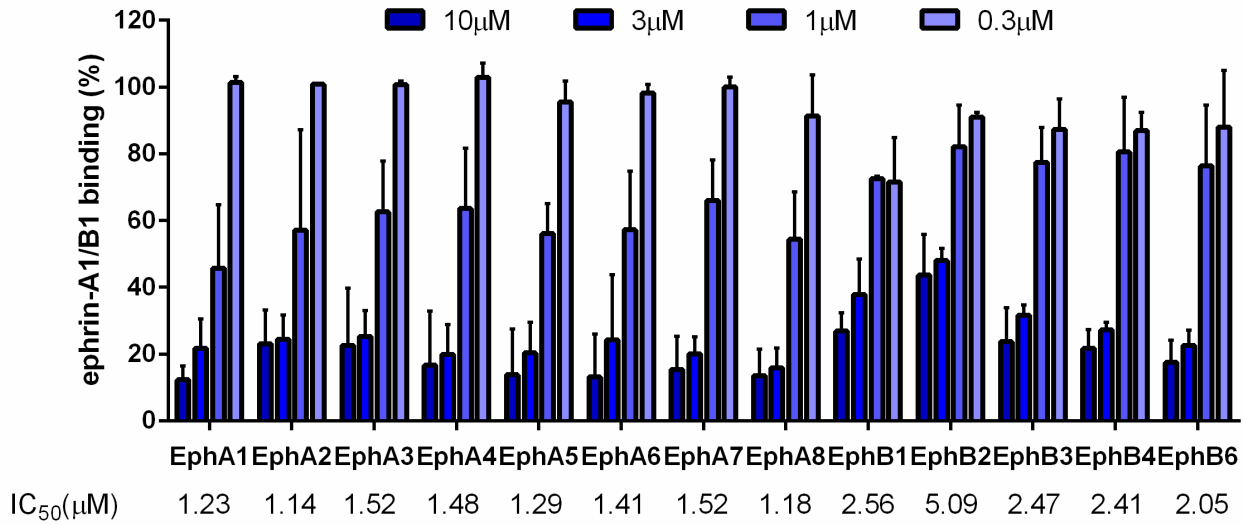


Figure 5. Binding of biotinylated ephrin-A1-Fc or ephrin-B1-Fc to EphA or EphB receptor ectodomains was dose-dependently inhibited by UniPR500. Data are the means of at least three independent experiments  $\pm$  st. dev.. IC<sub>50</sub> values are indicated at the bottom.

### Effect of targeting Eph/ephrin *in vitro*

#### UniPR500 increases insulin release from EndoC-βH1 cells

It was previously demonstrated that the activation of EphA5 by means of ephrin-A5-Fc inhibited insulin secretion upon glucose stimulation on murine MIN6 cell line and on primary isolated islets of both mice and humans [2]. Here, using a high-capacity, automated perfusion system, we checked if the incubation with the Eph antagonist UniPR500 was able to increase insulin secretion from EndoC-βH1 cells, a valid model of human beta cells [21], upon stimulation with 20mM glucose. As expected glucose stimulation doubled the basal insulin concentrations and this effect was enhanced by the inhibition of Eph receptors by means of UniPR500. Indeed 10µM UniPR500 significantly enhanced the insulin release by 5-fold upon glucose stimulation, confirming that Eph antagonism is a valuable strategy to improve glucose stimulated insulin secretion (GSIS) (Figure 6).

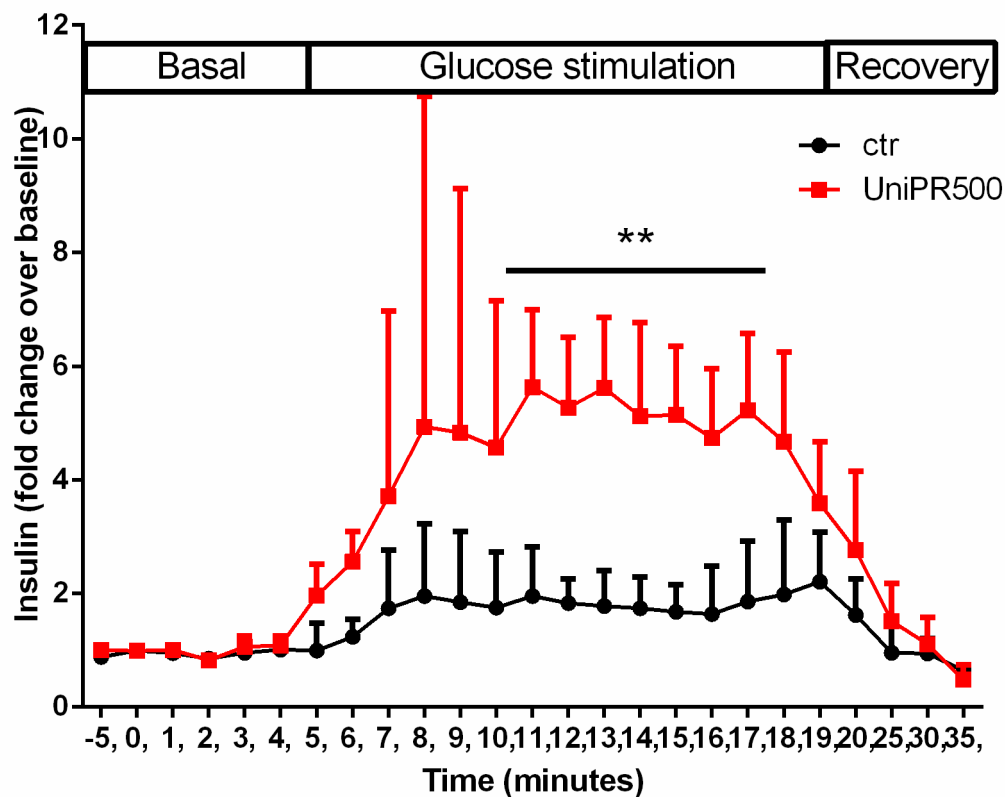


Figure 6. Release of insulin from EndoC- $\beta$ H1 perifusate. Glucose 20mM were added at minute 5 and removed at minute 25. Data are the means of at least three independent experiments  $\pm$  st. dev.. Two-way ANOVA followed by Bonferroni's post-test. \*\*,  $p < 0.01$ .

### UniPR500 does not interfere with classical targets involved in regulations of blood glucose levels

In order to confirm UniPR500 as a GSIS enhancer acting through the inhibition of Eph activation the compound was tested at 10  $\mu$ M on a panel of molecular targets known to be involved in the regulation of glucose levels (Table 1). UniPR500 resulted inactive both as an agonist or an antagonist on PPAR- $\gamma$  (target of glitazones, i.e. pioglitazone and rosiglitazone) and GLP-1 (target of GLP-1 agonists, i.e. exenatide and liraglutide) receptors. Furthermore UniPR500 did not inhibit DDP-4 (target of the gliptins, i.e. sitagliptin and vildagliptin) or PTP1B enzyme (target of the clinical candidate trodusquemine [22] and of the natural EphA2 antagonist lithocholic acid [23]) nor it interfered with functioning of the  $K_{ATP}$  ion channel (target of sulfonylureas, i.e. tolbutamide and glipizide).

Table 1. Selectivity panel for the Eph/ephrin antagonist UniPR500. The compound was tested at single dose (10  $\mu$ M) in triplicate. The biological activity of a reference standard for each target is also reported.

Target and test code	test	%inhibition or activation ( $\pm$ SD)	Standard IC <sub>50</sub> or EC <sub>50</sub>
GLP1, agonism 2181	Cellular functional assay GPCR/cAMP/HTRF	0.4 $\pm$ 0.2	GLP-1 (7-37), 0.052nM
GLP1, antagonism 2182	Cellular functional assay GPCR/cAMP/HTRF	13 $\pm$ 12	exendin-3(9-39), 5.7nM
PPAR- $\gamma$ , agonism 2771	Nuclear functional assay Coactivator recruitment/alphascreen	0.0 $\pm$ 0.0	Rosiglitazone, 190nM
PPAR- $\gamma$ , antagonism 2772	Nuclear functional assay Coactivator recruitment/alphascreen	-2.4 $\pm$ 6.8	GW9662, 91nM
PTP1B, inhibition 2593	Enzyme assay, fluorogenic substrate	-4.5 $\pm$ 0.7	(NH <sub>4</sub> ) <sub>6</sub> Mo <sub>7</sub> O <sub>24</sub> , 12nM
DPP IV, 2942	Enzyme assay, fluorogenic substrate	-3.3 $\pm$ 3.5	K579, 3nM
K <sub>ATP</sub> channel, 0165	Radioligand assay	7.0 $\pm$ 9.8	Glibenclamide, 0.25nM

### UniPR500 has a good physicochemical profile and it is orally available in mice

As our final aim was to administer UniPR500 *in vivo*, we next looked at key physicochemical properties of UniPR500 that could affect its oral bioavailability. We first evaluated physicochemical parameters affecting the absorption phase, such as lipophilicity (log D) and solubility (S), as well as the interaction with specific transporters that may enhance the uptake of UniPR500 in the bloodstream. As a second step, we focused our attention on the potential metabolic liability of UniPR500 by evaluating its stability in mouse plasma and liver. Table 2 summarizes the results of our *in vitro* ADMET profiling. UniPR500 showed log D (4.23) and kinetic solubility (52  $\mu$ M) values suitable for an oral absorption [24]. Furthermore, *in vitro* binding experiments indicated that UniPR500 interacts with the apical sodium-dependent bile acid transporter (ASBT), a key transporter expressed on the enterocytes of the terminal ileum which drives bile acids into the portal vein [25]. Next we evaluated *in vitro* the metabolic stability of UniPR500 by following its disappearance after incubation in murine plasma or in murine liver. In plasma, about 95% of UniPR500 was recovered after 24 h of incubation indicating that neither the amide linkage nor the iminohydroxyl group were subject to a significant chemical or enzymatic

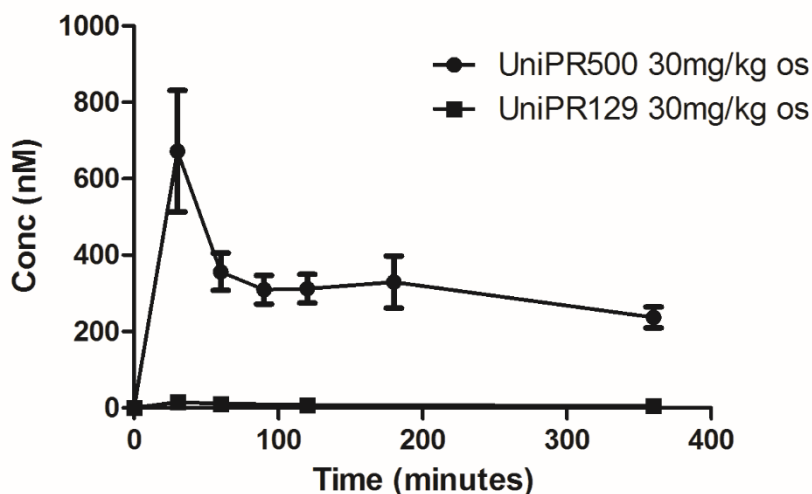
897  
898  
899 hydrolysis. In mouse liver S9 fraction, one of the available model to investigate oxidative metabolism, nearly 70  
900 % of UniPR500 was recovered unmodified after 1 h of incubation.  
901  
902

903 Table 2. Physicochemical properties, ASBT binding and *in vitro* stability of UniPR500  
904

Cpd	logD <sub>oct,7.4</sub>	solubility <sup>a</sup> ( $\mu$ M)	% ASBT binding <sup>b</sup>	% remaining compound in plasma <sup>c</sup>	% remaining compound in liver <sup>d</sup>
UniPR129	4.90 $\pm$ 0.15 <sup>e</sup>	31.8 $\pm$ 4.2 <sup>e</sup>	22.7 $\pm$ 2.4	98.3 $\pm$ 9.5 <sup>e</sup>	56 $\pm$ 5 <sup>e</sup>
UniPR500	4.23 $\pm$ 0.11 <sup>e</sup>	51.9 $\pm$ 4.4 <sup>e</sup>	92.6 $\pm$ 1.5	93.7 $\pm$ 11.3 <sup>e</sup>	70 $\pm$ 7 <sup>e</sup>

905  
906  
907  
908  
909  
910  
911 <sup>a</sup> From DMSO stock solution. <sup>b</sup> Percent bound at 10  $\mu$ M <sup>c</sup> Percent remaining after 24h of incubation, 37  $^{\circ}$ C <sup>d</sup>  
912 Percent remaining after 1 h incubation in the presence of a NADPH-regenerating system in liver S9 fraction <sup>e</sup> data  
913 from [19]. Data are the means of at least three independent experiments.  
914  
915  
916

917 Encouraged by these promising results we evaluated if UniPR500 was effectively bioavailable in mice by the oral  
918 route. After a single administration (30 mg/kg), the C<sub>max</sub> of UniPR500 was 0.7  $\mu$ M after 30 minutes, while its area  
919 under the curve (AUC<sub>0-t</sub>), a measure of systemic exposure to the compound, was equal to 573.1 ng/mL·h,  
920 indicating that UniPR500 could be used as a pharmacological tool in mice (Figure 7).  
921  
922  
923  
924



942 Figure 7 UniPR500 is orally bioavailable in mice. Plasma concentrations (nM) of UniPR500 over 6 hours time  
943 course after a single oral administration in male mice (30 mg/kg, os) are reported as obtained from HPLC/MS  
944 analysis. Data are the means of at least four independent experiments  $\pm$  SEM.  
945  
946  
947  
948  
949  
950  
951  
952

## Effect of targeting Eph/ephrin *in vivo*

### UniPR500 facilitates glucose adsorption in healthy and insulin-resistant mice

The bioavailability of the compound allowed us to evaluate the ability of UniPR500 to improve the glucose tolerance in healthy C57BL/6J mice. The vehicle (methocel) or the compound (30mg/kg) were orally administered to mice 30 minutes before challenge with glucose (2g/kg i.p.). In these conditions, UniPR500 significantly improved overall glucose tolerance and significantly reduced plasma glucose levels 60 minutes after glucose injection (Figure 8A). Fasting plasma glucose and insulin levels were not modified by UniPR500 treatment (Figure 8A, B) whereas 30 minutes after glucose injection, treated animals showed higher insulin concentrations (Figure 8B), confirming *in vitro* data that highlighted UniPR500 as GSIS enhancer. Taken together these data suggest that UniPR500 was able to improve glucose tolerance in healthy mice increasing GSIS without affecting basal glucose and insulin levels.

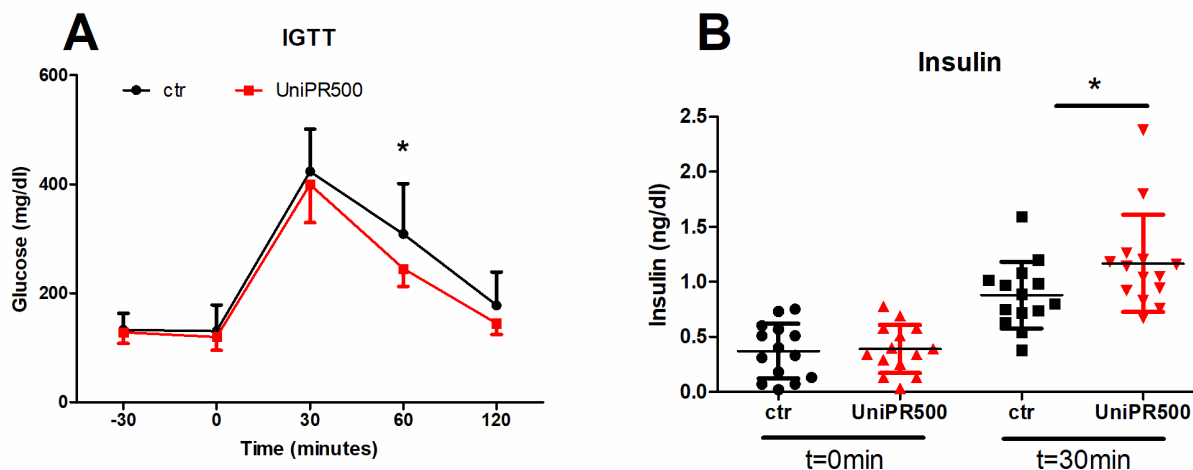


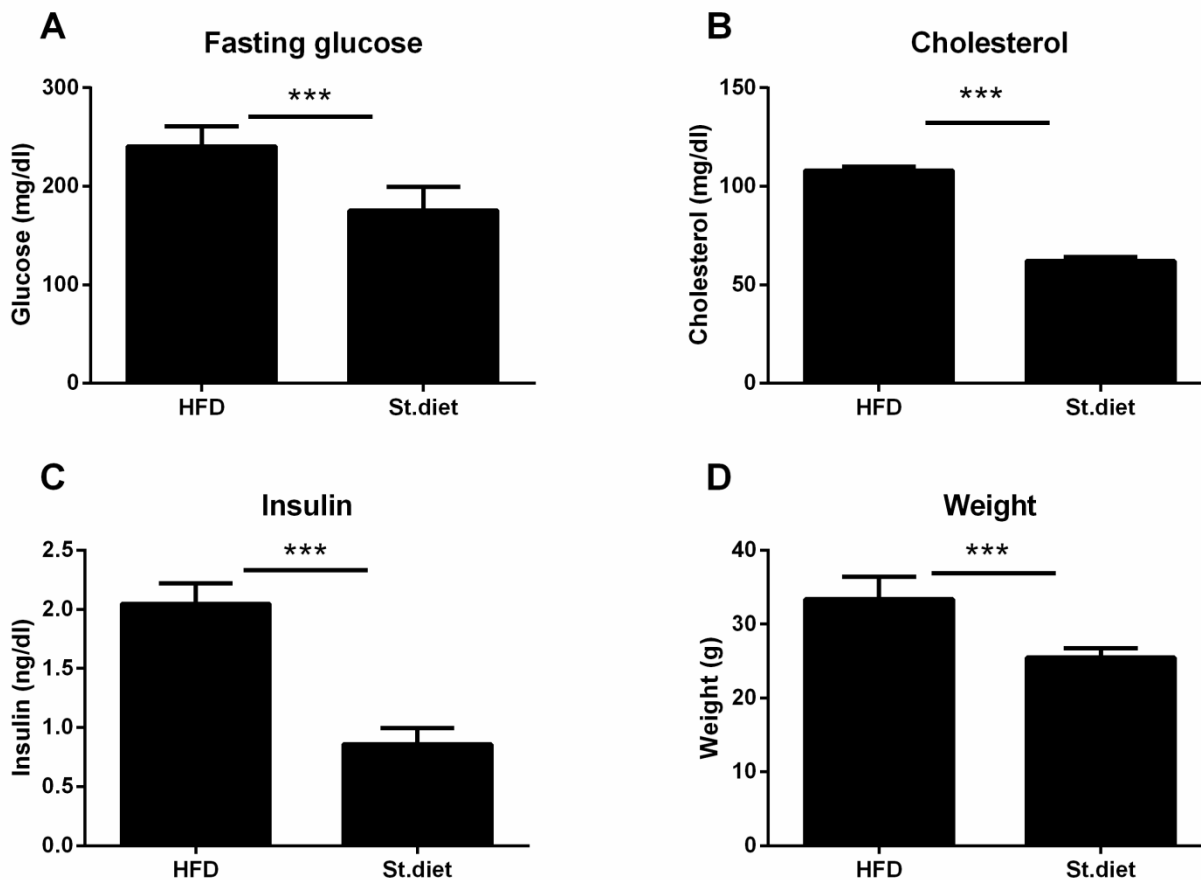
Figure 8. UniPR500 improves glucose tolerance test in mice

Glucose tolerance test (A) and plasma insulin levels (B) of male C57BL/6J mice before and after intraperitoneal injection of glucose (2g/kg). UniPR500 30mg/kg was administered 30 minutes before glucose injection. Data are the means  $\pm$  st. dev.. Two-way ANOVA followed by Bonferroni's post-test. \*,  $p < 0.05$ .

Afterwards we investigated if UniPR500 was able to control hyperglycaemia in two different non-genetic mouse models of impaired glucose tolerance: 1, the high-fat diet-fed mouse (HFD [13,14,26]) developing an early but persisting slight increase of fasting plasma glucose levels and a slow progressive increase of body weight and

1009  
1010  
1011 insulin levels mimicking the early phase of type 2 diabetes or a condition of insulin resistance; 2, HFD mouse +  
1012 low doses of streptozotocin injections, aiming at impairing insulin secretion mimicking a type 1 diabetes [27,28].

1013  
1014  
1015 The first model was obtained by using C57BL/6J mice fed for 10 weeks with High-Fat Diet (HFD, 60% calories from  
1016 fat, Mucedola, Milan, Italy) and orally administered with 30 mg/kg UniPR500, or methocel alone, during the last  
1017 2 weeks of the HFD treatment (e.g. 9<sup>th</sup> and the 10<sup>th</sup> week). Eight weeks of HFD-diet successfully yielded  
1018 hypercholesterolemic, hyperglycemic, hyperinsulinemic and overweight animals (Figure 9).  
1019  
1020



1021  
1022  
1023  
1024  
1025  
1026  
1027  
1028  
1029  
1030  
1031  
1032  
1033  
1034  
1035  
1036  
1037  
1038  
1039  
1040  
1041  
1042  
1043  
1044  
1045  
1046  
1047  
1048  
1049 *Figure 9. C57BL/6J mice were fed ad libitum for 8 weeks with standard diet (ctr) or High-Fat Diet (HFD) in order*  
1050 *to induce insulin resistance. Glucose (A), cholesterol (B), insulin fasting (C) levels and body weights (D) were*  
1051 *measured at the end of 8<sup>th</sup> week. Data are the means ± st.dev. T.test was performed \*\*\*, p<0.001.*

1052  
1053  
1054  
1055  
1056 Starting from the 9<sup>th</sup> week and until the end of the 10<sup>th</sup> week mice were divided in two group: treated group and  
1057 control group that were daily orally administered with 30mg/kg UniPR500 and methocel, respectively.  
1058  
1059  
1060  
1061  
1062  
1063  
1064

At the end of the treatment none of the previous parameters was reverted by UniPR500 treatment. In fact, HFD-mice treated with compound under investigation showed fasting cholesterol, glucose and weight levels comparable to HFD-mice (figure 10).

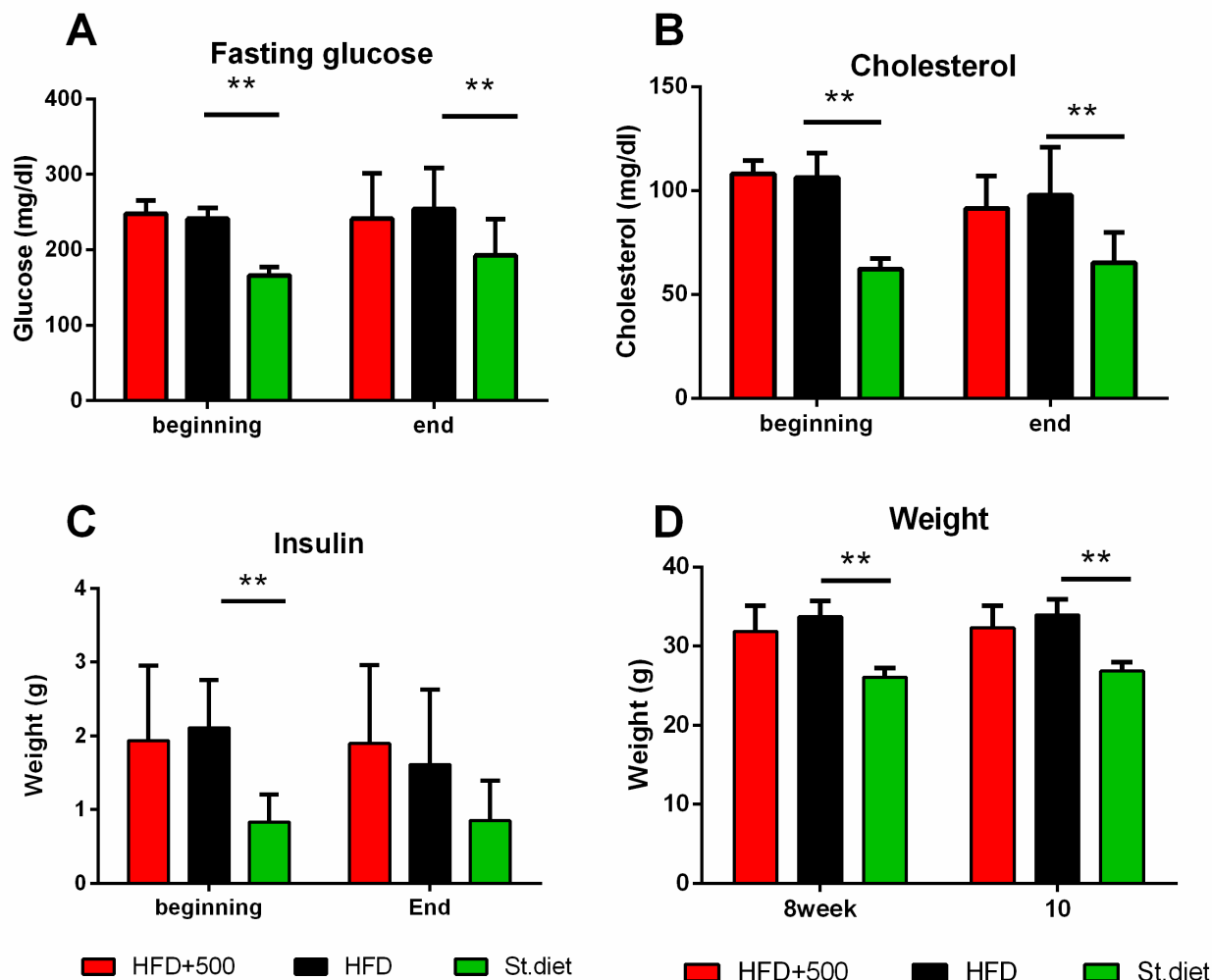


Figure 10. C57BL/6J standard mice (ctr) or insulin-resistant mice, fed with High-Fat Diet, were orally administered with 30 mg/kg UniPR500 (HFD+500) or methocel (HFD) for 14 days, from the 9<sup>th</sup> to the 10<sup>th</sup> week of HFD treatment. Data are the means  $\pm$  SD. Two-way ANOVA followed by Bonferroni's post-test compared HFD with other treatments. \*,  $p < 0.05$ , \*\*,  $p < 0.01$ , \*\*\*,  $p < 0.001$ . HFD=High Fat Diet mice, HFD+500=High Fat Diet mice + 14 days UniPR500 30m/kg/die os, ctr=standard diet mice.

The last administration of UniPR500 or vehicle took place 30 minutes before performing glucose tolerance test. As expected, in these conditions HFD-mice showed poor glucose tolerance when compared to mice fed with a

standard diet (figure 11A) despite the higher plasma insulin levels (Figure 11B) confirming that mice treated with HFD developed insulin-resistance. Nevertheless, HFD mice treated with UniPR500 showed a significant less severe glucose intolerance when compared to HFD-mice, particularly 60 and 120 minutes after glucose injection (figure 11A), also confirmed by AUC (figure 11C). Regarding plasma insulin HFD mice treated with UniPR500 appeared to have higher insulin plasma levels than HFD mice treated with vehicle, but the large scattering of data hamper further proper statistical consideration (figure 11B, D).

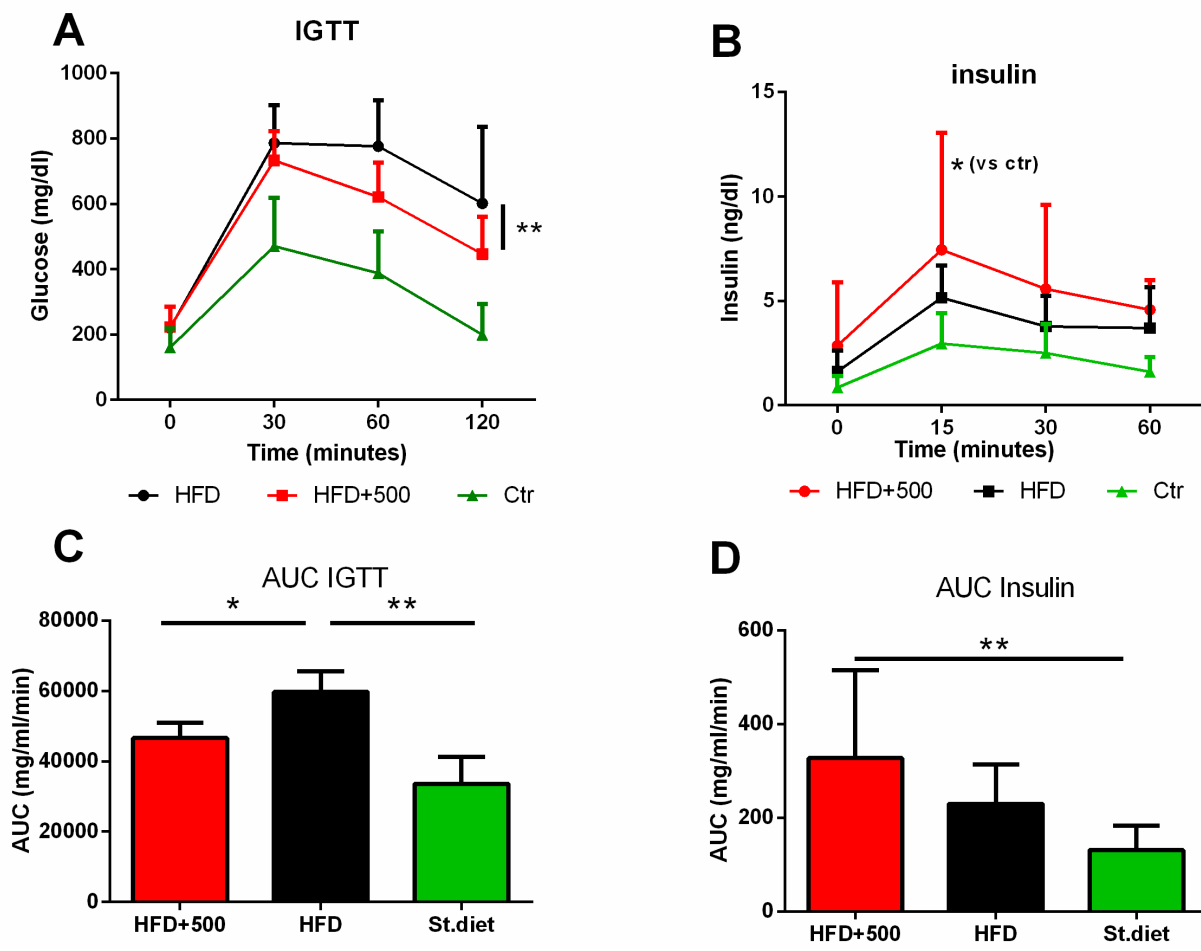


Figure 11. C57BL/6J mice, fed with High-Fat Diet, were orally administered with 30mg/kg UniPR500 (HFD+500) or methocel (HFD) for 14 days, from the 9<sup>th</sup> to the 10<sup>th</sup> week of HFD treatment. C57BL/6J mice fed with standard diet for ten weeks (ctr) were orally treated with methocel from the 9<sup>th</sup> to the 10<sup>th</sup> week.

Glucose tolerance test (A) and plasma insulin concentration (B) after intraperitoneal administration of glucose (2g/kg) 30 minutes after the last oral administration of 30mg/kg UniPR500 or methocel. Panels C and D represent AUC of glucose plasma levels and AUC of insulin plasma levels, respectively.

Data are the means ± st. dev.. Two-way ANOVA followed by Bonferroni's post-test (A, B) comparing HFD+500

1177  
1178  
1179 *with other treatments. One-way ANOVA followed by Dunnett's post-test for panels C and D, comparing HFD+500*  
1180 *with other treatments. \*, p<0.05, \*\*, p<0.01.*  
1181  
1182

### 1183 1184 **UniPR500 does not improve glucose tolerance test in streptozotocin-treated mice** 1185

1186 We finally asked if UniPR500 could improve glucose tolerance in a more severe model of diabetes induced by 5  
1187 consecutive administrations (days 1-5 of the experimental procedure) of a low dose of streptozotocin (40mg/kg  
1188 i.p. 1 x day, 5 consecutive days) followed by HFD diet for 6 weeks (days 8 – 50 of the experimental procedure).  
1189 This model is not univocally described by Authors as a model of type 1 diabetes [14,28,29], but our histological  
1190 findings showed an extensive pancreatic damage compromising  $\beta$ -cell function. According to the histopathological  
1191 features, no significant differences emerged between the streptozotocin-HFD mice treated with UniPR500 and  
1192 streptozotocin-HFD untreated mice; both groups showed endocrine pancreatic injuries, islet cells vacuolation  
1193 and lymphocytes infiltration, indicative of Insulin-Dependent Diabetes Mellitus, mild or severe degenerative  
1194 changes (steatosis) in the liver, slight focal interstitial inflammation in kidneys (supplementary material).  
1195  
1196  
1197  
1198  
1199

1200 As expected, mice showed high fasting glucose and cholesterol plasma concentrations together with significantly  
1201 higher body weights when compared with animals fed with standard diet and not receiving streptozotocin  
1202 injections (data not shown). At 37<sup>th</sup> day of the experimental procedure, streptozotocin + HFD mice were  
1203 randomly divided in 2 groups and daily treated with 30mg/kg UniPR500 or methocel respectively. Compound  
1204 administration did not modify fasting glucose or cholesterol levels after 14 days of treatment neither changed  
1205 weight when compared with mice treated only with vehicle (data not shown).  
1206  
1207  
1208

1209 At the 50<sup>th</sup> day the last administration of UniPR500 30mg/kg or Methocel was done 30 minutes before  
1210 performing IGTT on streptozotocin + HFD mice (mice fed with standard diet are used as internal control).  
1211 Streptozotocin + HFD mice showed a very poor glucose tolerance highlighted by an AUC nearly 4-fold higher than  
1212 control animals. The subchronic treatment with 30mg/kg UniPR500 failed to improve glucose tolerance in these  
1213 mice and the pancreas histological analysis of these animals could help to explain this data (figure 12). In fact in  
1214 these mice pancreas resulted severely damage suggesting  $\beta$ -cell function impairment. As expected by a GSIS  
1215 enhancer, since UniPR500 improves glucose tolerance through the increase of insulin release from healthy  $\beta$ -  
1216 cells, it can not act if these cells are damaged and no longer working, a condition that reflect a type 1 diabetes  
1217 rather than a type 2 diabetes or I/R.  
1218  
1219  
1220  
1221  
1222  
1223  
1224  
1225  
1226  
1227  
1228  
1229  
1230  
1231  
1232

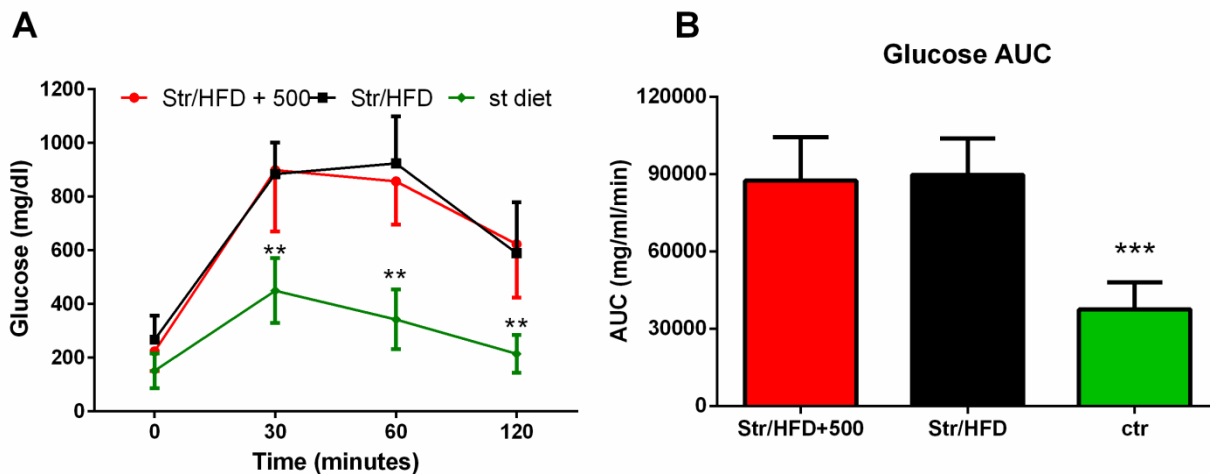


Figure 12. UniPR500 does not modify glucose tolerance of streptozotocin/HFD mice

C57BL/6J mice were injected with streptozotocin 40mg/kg i.p. and fed ad libitum for 42 days with High-Fat Diet. UniPR500 30mg/kg or Methocel were orally administered for 14 days from day 37 to day 50. **A**, Glucose tolerance test after intraperitoneal administration of glucose (2g/kg) 30 minutes after the last oral administration of 30mg/kg UniPR500 or methocel at the end of treatment **B**, AUC of panel **A**. Data are the means  $\pm$  st. dev.. Two-way ANOVA followed by Bonferroni's post-test (**A**) comparing all the treatments, \*\*,  $p < 0.01$  for standard diet vs other treatments. One-way ANOVA followed by Dunnett's test for panels **B**.\*\*\*, for standard diet vs other treatments.

## DISCUSSION

Eph/ephrin system is an emerging target for cancer therapy and different pharmacological approaches were developed or are under development by using proteins, peptides, antibodies or small molecules including PPI-inhibitors and kinase inhibitors [7]. In this context, we have recently started a drug discovery program aimed at finding PPI inhibitors targeting Eph/ephrin interaction identifying lithocholic acid (LCA) as hit compound during a screening campaign. Through an iterative lead optimization phase based on molecular simulations [9] synthesis and pharmacological analysis [19], we developed new derivatives endowed with better potency, efficacy, chemico-physical properties and bioavailability [10]. UniPR500 represents the most advanced LCA derivative developed so far targeting the Eph/ephrin interface, also in light of its high selectivity versus the Eph receptors. This compound failed to interact with several targets involved in the control of glucose homeostasis

1289  
1290  
1291 i.e. PPAR- $\gamma$ ; GLP-1; DDP-4; PTP1B enzyme KATP ion channel and TGR5 (GPBAR1), the critical G-protein coupled  
1292 receptor activated by LCA and close analogues [18]  
1293

1294  
1295 Even if Eph/ephrin targeting was primarily addressed at the discovery of new drugs useful for cancer therapy  
1296 and many proof-of concepts support its efficacy [29–33], its usefulness is going to be studied also in other fields  
1297 including ALS [34], nerve regeneration and diabetes [35]. As for the latter case Jain et al showed that kinase  
1298 inhibitors of the EphA receptors increased GSIS both in *in vitro* and in *in vivo* studies [6]. In fact the inhibition of  
1299 EphA5 forward signaling was shown to increase GSIS, as well the activation of ephrin-A reverse signaling [2]. In  
1300 this context it is not surprising that pharmacological blockade of EphA receptors by means of a kinase inhibitor  
1301 resulted in increased GSIS [6].  
1302

1303  
1304 Here we tested the *in vitro* and *in vivo* efficacy of UniPR500, a new PPI inhibitor targeting Eph-ephrin  
1305 interaction. It is worth to note that kinase inhibitors are able to block the forward signaling only whereas the  
1306 PPI-inhibitor UniPR500 used in this study can block both the forward and the reverse signaling. The behavior of  
1307 a UniPR500 as GSIS enhancer is not obvious since it may increase GSIS by blocking forward signaling controlled  
1308 by EphA5 but it may also reduce GSIS by inhibiting the reverse signaling controlled by ephrin-A5.  
1309

1310  
1311 In the previous study [6] a roughly 2-fold increase of insulin secretion upon treatment with Eph kinase  
1312 inhibitors on MIN6 or mice pancreatic islet cells was described. In our study we used the innovative technique  
1313 of dynamic perfusion to study real time insulin secretion from human EndoC- $\beta$ H1 cells [36]. We showed that  
1314 GSIS peaked between 10 to 20 minutes after glucose stimulation and completely finished after 30 minutes. In  
1315 our model UniPR500 induced an up to 5-fold increased insulin release which prompted us to evaluate further  
1316 this compound in *in vivo* models of diabetes.  
1317

1318  
1319 We next studied the effect of UniPR500 on glucose tolerance in healthy mice and, according to our data on the  
1320 dynamic perfusion model, we found a significant increase in insulin secretion and glucose tolerance. Overall,  
1321 this further confirms the efficacy of Eph signaling inhibition as a valid strategy in GSIS potentiation. However  
1322 UniPR500 appeared less effective than kinase inhibitors [6] as GSIS enhancer in mice and consequently the  
1323 improvement of glucose tolerance turned out to be minor. The apparently lower efficacy of UniPR500 may be  
1324 explained by the use of different doses or by considering the different mechanism of action of this molecule in  
1325 comparison to kinase inhibitors. As mentioned before, kinase inhibitors block only Eph forward signaling whilst  
1326 a PPI-inhibitor like UniPR500 can reduce insulin release by inhibiting the reverse signaling. In the future may be  
1327 interesting to evaluate in the same model the effect of the recombinant EphA5-Fc in comparison to Eph kinase  
1328 inhibitors and Eph/ephrin antagonists. Indeed, EphA5-Fc may be able to block EphA5 forward signaling as  
1329  
1330  
1331  
1332  
1333  
1334  
1335  
1336  
1337  
1338  
1339  
1340  
1341  
1342  
1343  
1344

1345  
1346  
1347 kinase inhibitor, but also able to activate ephrin-A5 reverse signaling at the same time. In this view EphA5-Fc  
1348 may be even more effective than kinase inhibitors as GSIS enhancer and glucose tolerance improver.  
1349

1350  
1351 In addition, we studied for the first time the effect of Eph/ephrin targeting on glucose tolerance in a non-  
1352 genetic mouse model of insulin resistance, where UniPR500 treatment allowed a faster recovery from  
1353 hyperglycemia. Since no data are available with kinase inhibitors, future studies aimed at evaluating their  
1354 efficacy could be very interesting.  
1355  
1356

1357  
1358 Finally, as expected by a GSIS enhancer, UniPR500 failed to improve glucose tolerance when IGTT was  
1359 performed in a condition where mice pancreatic function was severely compromised. New approaches are  
1360 under investigations to control autoimmune diabetes by modulating the immune response through  
1361 phosphoinositide 3-kinase-γ inhibitors PTPN22 [37], carbamazepine [38], CCL4 administration [39] or Beta cells  
1362 replacement [40].  
1363  
1364  
1365

## 1366 CONCLUSIONS

1367  
1368 Although further studies are needed to clarify if an alteration of Eph/ephrin system affects pancreas of T2D  
1369 patients, these data demonstrate that Eph targeting agents are new and promising insulin enhancers,  
1370 potentially devoid of hypoglycaemic side effect thanks to their action on GSIS rather than on basal insulin  
1371 release. Moreover, the relative low expression profile of Eph/ephrin system in adult tissues may ensure for this  
1372 new class of drugs a satisfactory safety profile in clinical use. Nevertheless given the prominent role played by  
1373 this system during embryogenesis [41], further studies on possible teratogenic effects of these compounds are  
1374 needed. Interestingly, the literature data highlighted the involvement of Eph/ephrin signaling in vascular and  
1375 nerve injuries, as well as in the neuropathic pain transmission [42,43], all diabetes comorbidities. Therefore,  
1376 further investigations are essential to determine the complete pharmacological/toxicological profile of action  
1377 of this new class of Eph/ephrin antagonists after chronic administration.  
1378  
1379  
1380  
1381  
1382  
1383  
1384  
1385

## 1386 REFERENCES

- 1387  
1388  
1389 [1] M.J. Luther, A. Hauge-Evans, K.L.A. Souza, A. Jörns, S. Lenzen, S.J. Persaud, P.M. Jones, MIN6 beta-cell-  
1390 beta-cell interactions influence insulin secretory responses to nutrients and non-nutrients, *Biochem.*  
1391 *Biophys. Res. Commun.* 343 (2006) 99–104. doi:10.1016/j.bbrc.2006.02.003.  
1392 [2] I. Konstantinova, G. Nikolova, M. Ohara-Imaizumi, P. Meda, T. Kucera, K. Zarbalis, W. Wurst, S.  
1393 Nagamatsu, E. Lammert, EphA-Ephrin-A-mediated beta cell communication regulates insulin secretion  
1394 from pancreatic islets, *Cell.* 129 (2007) 359–370. doi:10.1016/j.cell.2007.02.044.  
1395 [3] E.B. Pasquale, Eph-ephrin bidirectional signaling in physiology and disease, *Cell.* 133 (2008) 38–52.  
1396 doi:10.1016/j.cell.2008.03.011.  
1397  
1398  
1399  
1400

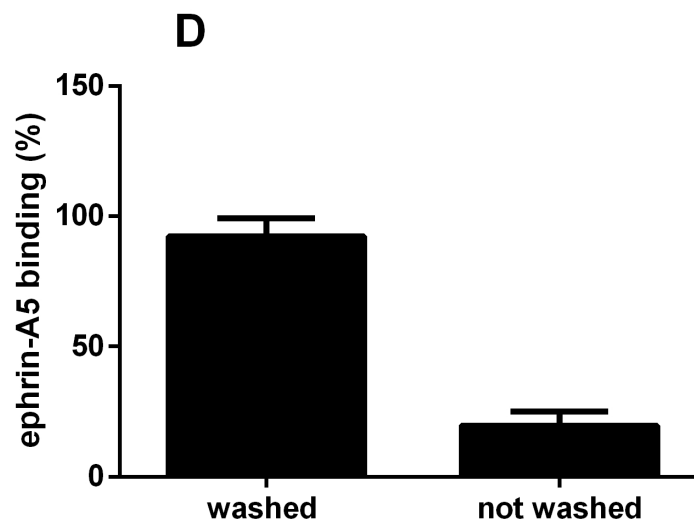
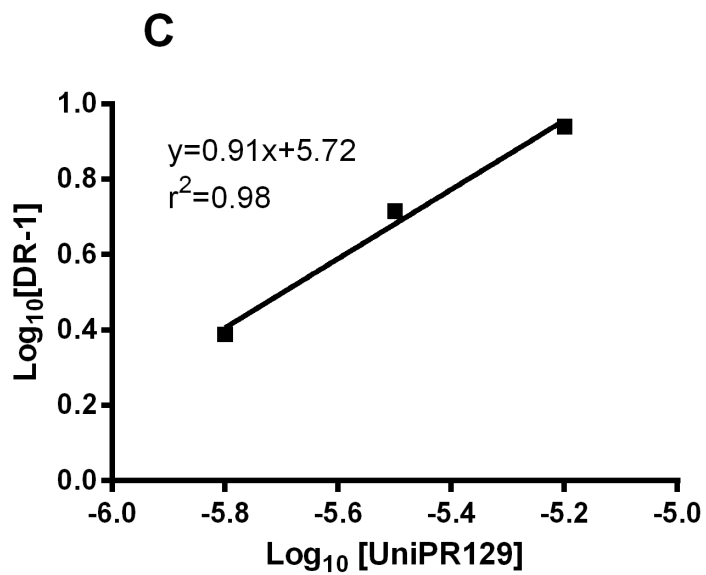
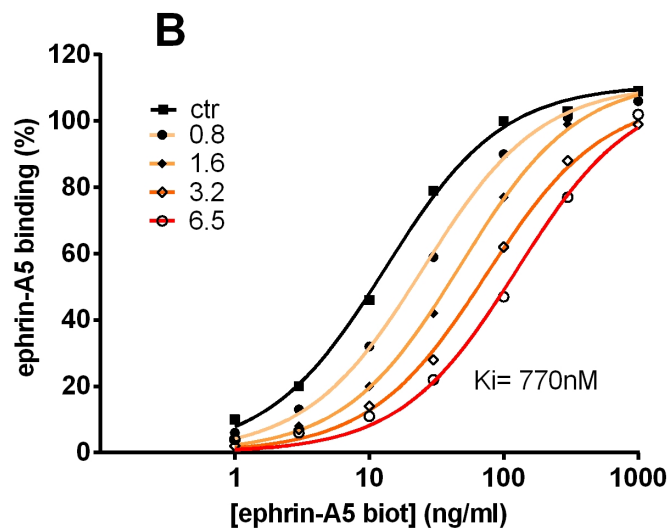
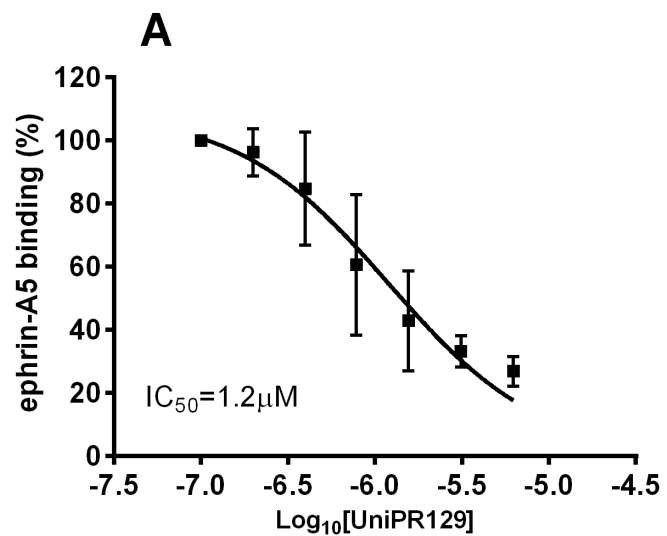
- 1401  
1402  
1403  
1404  
1405  
1406  
1407  
1408  
1409  
1410  
1411  
1412  
1413  
1414  
1415  
1416  
1417  
1418  
1419  
1420  
1421  
1422  
1423  
1424  
1425  
1426  
1427  
1428  
1429  
1430  
1431  
1432  
1433  
1434  
1435  
1436  
1437  
1438  
1439  
1440  
1441  
1442  
1443  
1444  
1445  
1446  
1447  
1448  
1449  
1450  
1451  
1452  
1453  
1454  
1455  
1456
- [4] G. Mellitzer, Q. Xu, D.G. Wilkinson, Eph receptors and ephrins restrict cell intermingling and communication, *Nature*. 400 (1999) 77–81. doi:10.1038/21907.
  - [5] C. Dorrell, J. Schug, C.F. Lin, P.S. Canaday, A.J. Fox, O. Smirnova, R. Bonnah, P.R. Streeter, C.J. Stoeckert, K.H. Kaestner, M. Grompe, Transcriptomes of the major human pancreatic cell types, *Diabetologia*. 54 (2011) 2832–2844. doi:10.1007/s00125-011-2283-5.
  - [6] R. Jain, D. Jain, Q. Liu, B. Bartosinska, J. Wang, D. Schumann, S.G. Kauschke, P. Eickelmann, L. Piemonti, N.S. Gray, E. Lammert, Pharmacological inhibition of Eph receptors enhances glucose-stimulated insulin secretion from mouse and human pancreatic islets, *Diabetologia*. 56 (2013) 1350–1355. doi:10.1007/s00125-013-2877-1.
  - [7] A. Lodola, C. Giorgio, M. Incerti, I. Zanotti, M. Tognolini, Targeting Eph/ephrin system in cancer therapy, *Eur. J. Med. Chem.* 142 (2017) 152–162. doi:10.1016/j.ejmech.2017.07.029.
  - [8] I. Hassan-Mohamed, C. Giorgio, M. Incerti, S. Russo, D. Pala, E.B. Pasquale, I. Zanotti, P. Vicini, E. Barocelli, S. Rivara, M. Mor, A. Lodola, M. Tognolini, UniPR129 is a competitive small molecule Eph-ephrin antagonist blocking in vitro angiogenesis at low micromolar concentrations, *Br. J. Pharmacol.* 171 (2014) 5195–5208. doi:10.1111/bph.12669.
  - [9] S. Russo, D. Callegari, M. Incerti, D. Pala, C. Giorgio, J. Brunetti, L. Bracci, P. Vicini, E. Barocelli, L. Capoferri, S. Rivara, M. Tognolini, M. Mor, A. Lodola, Exploiting Free-Energy Minima to Design Novel EphA2 Protein-Protein Antagonists: From Simulation to Experiment and Return, *Chem. Weinh. Bergstr. Ger.* 22 (2016) 8048–8052. doi:10.1002/chem.201600993.
  - [10] M. Tognolini, M. Incerti, D. Pala, S. Russo, R. Castelli, I. Hassan-Mohamed, C. Giorgio, A. Lodola, Target hopping as a useful tool for the identification of novel EphA2 protein-protein antagonists, *ChemMedChem*. 9 (2014) 67–72. doi:10.1002/cmdc.201300305.
  - [11] R. Castelli, M. Tognolini, F. Vacondio, M. Incerti, D. Pala, D. Callegari, S. Bertoni, C. Giorgio, I. Hassan-Mohamed, I. Zanotti, A. Bugatti, M. Rusnati, C. Festuccia, S. Rivara, E. Barocelli, M. Mor, A. Lodola,  $\Delta(5)$ -Cholenoyl-amino acids as selective and orally available antagonists of the Eph-ephrin system, *Eur. J. Med. Chem.* 103 (2015) 312–324. doi:10.1016/j.ejmech.2015.08.048.
  - [12] P. Ravassard, Y. Hazhouz, S. Pechberty, E. Bricout-Neveu, M. Armanet, P. Czernichow, R. Scharfmann, A genetically engineered human pancreatic  $\beta$  cell line exhibiting glucose-inducible insulin secretion, *J. Clin. Invest.* 121 (2011) 3589–3597. doi:10.1172/JCI58447.
  - [13] X.-Y. Zeng, Y.-P. Wang, J. Cantley, T.J. Iseli, J.C. Molero, B.D. Hegarty, E.W. Kraegen, Y. Ye, J.-M. Ye, Oleonic acid reduces hyperglycemia beyond treatment period with Akt/FoxO1-induced suppression of hepatic gluconeogenesis in type-2 diabetic mice, *PloS One*. 7 (2012) e42115. doi:10.1371/journal.pone.0042115.
  - [14] E.R. Gilbert, Z. Fu, D. Liu, Development of a nongenetic mouse model of type 2 diabetes, *Exp. Diabetes Res.* 2011 (2011) 416254. doi:10.1155/2011/416254.
  - [15] O. Arunlakshana, H.O. Schild, Some quantitative uses of drug antagonists, *Br. J. Pharmacol. Chemother.* 14 (1959) 48–58.
  - [16] S. Russo, M. Incerti, M. Tognolini, R. Castelli, D. Pala, I. Hassan-Mohamed, C. Giorgio, F. De Franco, A. Gioiello, P. Vicini, E. Barocelli, S. Rivara, M. Mor, A. Lodola, Synthesis and structure-activity relationships of amino acid conjugates of cholanolic acid as antagonists of the EphA2 receptor, *Mol. Basel Switz.* 18 (2013) 13043–13060. doi:10.3390/molecules181013043.
  - [17] C. Thomas, A. Gioiello, L. Noriega, A. Strehle, J. Oury, G. Rizzo, A. Macchiarulo, H. Yamamoto, C. Matak, M. Pruzanski, R. Pellicciari, J. Auwerx, K. Schoonjans, TGR5-mediated bile acid sensing controls glucose homeostasis, *Cell Metab.* 10 (2009) 167–177. doi:10.1016/j.cmet.2009.08.001.
  - [18] A. Macchiarulo, A. Gioiello, C. Thomas, T.W.H. Pols, R. Nuti, C. Ferrari, N. Giacchè, F. De Franco, M. Pruzanski, J. Auwerx, K. Schoonjans, R. Pellicciari, Probing the Binding Site of Bile Acids in TGR5, *ACS Med. Chem. Lett.* 4 (2013) 1158–1162. doi:10.1021/ml400247k.

- 1457  
1458  
1459  
1460  
1461  
1462  
1463  
1464  
1465  
1466  
1467  
1468  
1469  
1470  
1471  
1472  
1473  
1474  
1475  
1476  
1477  
1478  
1479  
1480  
1481  
1482  
1483  
1484  
1485  
1486  
1487  
1488  
1489  
1490  
1491  
1492  
1493  
1494  
1495  
1496  
1497  
1498  
1499  
1500  
1501  
1502  
1503  
1504  
1505  
1506  
1507  
1508  
1509  
1510  
1511  
1512
- [19] M. Incerti, S. Russo, D. Callegari, D. Pala, C. Giorgio, I. Zanotti, E. Barocelli, P. Vicini, F. Vacondio, S. Rivara, R. Castelli, M. Tognolini, A. Lodola, *Metadynamics for Perspective Drug Design: Computationally Driven Synthesis of New Protein-Protein Interaction Inhibitors Targeting the EphA2 Receptor*, *J. Med. Chem.* 60 (2017) 787–796. doi:10.1021/acs.jmedchem.6b01642.
- [20] H. Duboc, Y. Taché, A.F. Hofmann, *The bile acid TGR5 membrane receptor: from basic research to clinical application*, *Dig. Liver Dis. Off. J. Ital. Soc. Gastroenterol. Ital. Assoc. Study Liver.* 46 (2014) 302–312. doi:10.1016/j.dld.2013.10.021.
- [21] V.G. Tsonkova, F.W. Sand, X.A. Wolf, L.G. Grunnet, A. Kirstine Ringgaard, C. Ingvorsen, L. Winkel, M. Kalisz, K. Dalgaard, C. Bruun, J.J. Fels, C. Helgstrand, S. Hastrup, F.K. Öberg, E. Vernet, M.P.B. Sandrini, A.C. Shaw, C. Jessen, M. Grønberg, J. Hald, H. Willenbrock, D. Madsen, R. Wernersson, L. Hansson, J.N. Jensen, A. Plesner, T. Alanentalo, M.B.K. Petersen, A. Grapin-Botton, C. Honoré, J. Ahnfelt-Rønne, J. Hecksher-Sørensen, P. Ravassard, O.D. Madsen, C. Rescan, T. Frogne, *The EndoC-βH1 cell line is a valid model of human beta cells and applicable for screenings to identify novel drug target candidates*, *Mol. Metab.* (2017). doi:10.1016/j.molmet.2017.12.007.
- [22] H. Cho, *Protein tyrosine phosphatase 1B (PTP1B) and obesity*, *Vitam. Horm.* 91 (2013) 405–424. doi:10.1016/B978-0-12-407766-9.00017-1.
- [23] H.-B. He, L.-X. Gao, Q.-F. Deng, W.-P. Ma, C.-L. Tang, W.-W. Qiu, J. Tang, J.-Y. Li, J. Li, F. Yang, *Synthesis and biological evaluation of 4,4-dimethyl lithocholic acid derivatives as novel inhibitors of protein tyrosine phosphatase 1B*, *Bioorg. Med. Chem. Lett.* 22 (2012) 7237–7242. doi:10.1016/j.bmcl.2012.09.040.
- [24] E.H. Kerns, L. Di, Chapter 5 - Lipophilicity, in: *Drug- Prop. Concepts Struct. Des. Methods*, Academic Press, San Diego, 2008: pp. 43–47. doi:10.1016/B978-012369520-8.50006-1.
- [25] P.A. Dawson, *Role of the intestinal bile acid transporters in bile acid and drug disposition*, *Handb. Exp. Pharmacol.* (2011) 169–203. doi:10.1007/978-3-642-14541-4\_4.
- [26] M.S. Winzell, B. Ahrén, *The high-fat diet-fed mouse: a model for studying mechanisms and treatment of impaired glucose tolerance and type 2 diabetes*, *Diabetes.* 53 Suppl 3 (2004) S215-219.
- [27] *Rodent models of streptozotocin-induced diabetic nephropathy (Methods in Renal Research) - TESCH - 2007 - Nephrology - Wiley Online Library*, (n.d.). <https://onlinelibrary.wiley.com/doi/full/10.1111/j.1440-1797.2007.00796.x> (accessed June 7, 2018).
- [28] M.C. Deeds, J.M. Anderson, A.S. Armstrong, D.A. Gastineau, H.J. Hiddinga, A. Jahangir, N.L. Eberhardt, Y.C. Kudva, *Single dose streptozotocin-induced diabetes: considerations for study design in islet transplantation models*, *Lab. Anim.* 45 (2011) 131–140. doi:10.1258/la.2010.010090.
- [29] M. Damelin, A. Bankovich, A. Park, J. Aguilar, W. Anderson, M. Santaguida, M. Aujay, S. Fong, K. Khandke, V. Pulito, E. Ernstoff, P. Escarpe, J. Bernstein, M. Pysz, W. Zhong, E. Upešlacis, J. Lucas, J. Lucas, T. Nichols, K. Loving, O. Foord, J. Hampl, R. Stull, F. Barletta, H. Falahatpisheh, P. Sapra, H.-P. Gerber, S.J. Dylla, *Anti-*EFNA4* Calicheamicin Conjugates Effectively Target Triple-Negative Breast and Ovarian Tumor-Initiating Cells to Result in Sustained Tumor Regressions*, *Clin. Cancer Res. Off. J. Am. Assoc. Cancer Res.* 21 (2015) 4165–4173. doi:10.1158/1078-0432.CCR-15-0695.
- [30] C.M. Annunziata, E.C. Kohn, P. LoRusso, N.D. Houston, R.L. Coleman, M. Buzoianu, G. Robbie, R. Lechleider, *Phase 1, open-label study of MEDI-547 in patients with relapsed or refractory solid tumors*, *Invest. New Drugs.* 31 (2013) 77–84. doi:10.1007/s10637-012-9801-2.
- [31] A. El-Khoueiry, B. Gitlitz, S. Cole, D. Tsao-Wei, A. Goldkorn, D. Quinn, H.J. Lenz, J. Nieva, T. Dorff, M. Oswald, J. Berg, X. Menendez, K. Karakozian, V. Krasnoperov, R. Liu, J. Thomas, S. Groshen, P. Gill, *A first-in-human phase I study of sEphB4-HSA in patients with advanced solid tumors with expansion at the maximum tolerated dose (MTD) or recommended phase II dose (RP2D)*, *Eur. J. Cancer.* 69 (2016) S11. doi:10.1016/S0959-8049(16)32623-5.
- [32] C. Hugen, G. Morrison, P. Gill, A. El-Khoueiry, D. Tsao-Wei, S. Groshen, Y. Xu, T. Xu, N. Kossari, B. Kao, J. Wei, H. Rochefort, Y.C. Tai, A. Goldkorn, *Circulating tumor cell analysis in a first-in-human phase I study of*

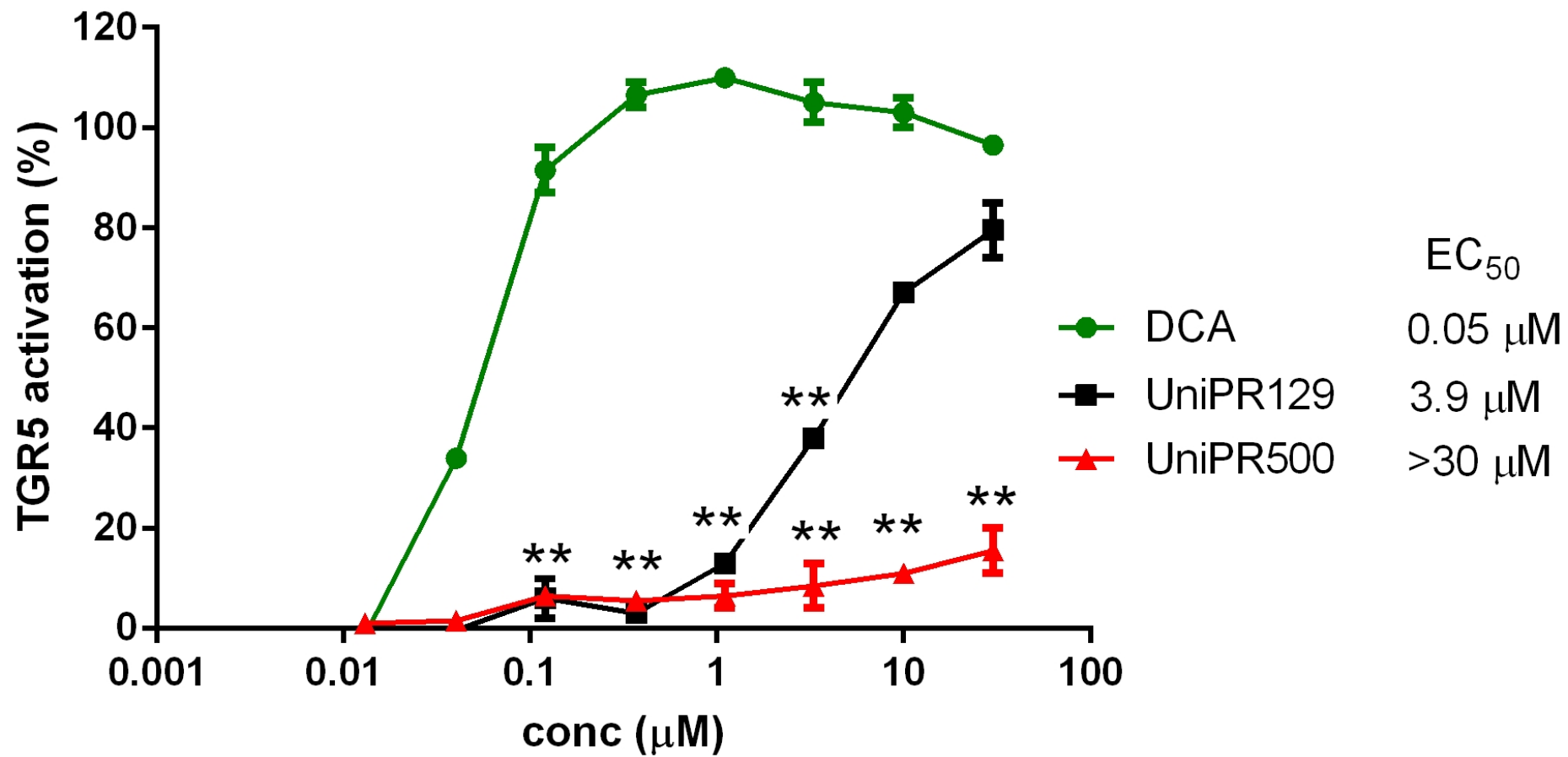
- 1513  
1514  
1515 sEphB4-HSA, an inhibitor of EphrinB2-EphB4 signaling, *Eur. J. Cancer.* 69 (2016) S126–S127.  
1516 doi:10.1016/S0959-8049(16)32976-8.  
1517 [33] A.F. Salem, S. Wang, S. Billet, J.-F. Chen, P. Udompholkul, L. Gambini, C. Baggio, H.-R. Tseng, E.M. Posadas,  
1518 N.A. Bhowmick, M. Pellecchia, Reduction of Circulating Cancer Cells and Metastases in Breast-Cancer  
1519 Models by a Potent EphA2-Agonistic Peptide-Drug Conjugate, *J. Med. Chem.* 61 (2018) 2052–2061.  
1520 doi:10.1021/acs.jmedchem.7b01837.  
1521 [34] B. Wu, S.K. De, A. Kulinich, A.F. Salem, J. Koeppen, R. Wang, E. Barile, S. Wang, D. Zhang, I. Ethell, M.  
1522 Pellecchia, Potent and Selective EphA4 Agonists for the Treatment of ALS, *Cell Chem. Biol.* 24 (2017) 293–  
1523 305. doi:10.1016/j.chembiol.2017.01.006.  
1524 [35] M. Tognolini, I. Hassan-Mohamed, C. Giorgio, I. Zanotti, A. Lodola, Therapeutic perspectives of Eph-ephrin  
1525 system modulation, *Drug Discov. Today.* 19 (2014) 661–669. doi:10.1016/j.drudis.2013.11.017.  
1526 [36] V.G. Tsonkova, F.W. Sand, X.A. Wolf, L.G. Grunnet, A. Kirstine Ringgaard, C. Ingvorsen, L. Winkel, M.  
1527 Kalisz, K. Dalgaard, C. Bruun, J.J. Fels, C. Helgstrand, S. Hastrup, F.K. Öberg, E. Vernet, M.P.B. Sandrini, A.C.  
1528 Shaw, C. Jessen, M. Grønberg, J. Hald, H. Willenbrock, D. Madsen, R. Wernersson, L. Hansson, J.N. Jensen,  
1529 A. Plesner, T. Alanentalo, M.B.K. Petersen, A. Grapin-Botton, C. Honoré, J. Ahnfelt-Rønne, J. Hecksher-  
1530 Sørensen, P. Ravassard, O.D. Madsen, C. Rescan, T. Frogne, The EndoC-βH1 cell line is a valid model of  
1531 human beta cells and applicable for screenings to identify novel drug target candidates, *Mol. Metab.* 8  
1532 (2018) 144–157. doi:10.1016/j.molmet.2017.12.007.  
1533 [37] G. Prezioso, L. Comegna, G. Di, S. Franchini, F. Chiarelli, A. Blasetti, C1858T Polymorphism of Protein  
1534 Tyrosine Phosphatase Non-receptor Type 22 (PTPN22): an eligible target for prevention of type 1  
1535 diabetes?, *Expert Rev. Clin. Immunol.* 13 (2017) 189–196. doi:10.1080/1744666X.2017.1266257.  
1536 [38] J.T.C. Lee, I. Shanina, Y.N. Chu, M.S. Horwitz, J.D. Johnson, Carbamazepine, a beta-cell protecting drug,  
1537 reduces type 1 diabetes incidence in NOD mice, *Sci. Rep.* 8 (2018) 4588. doi:10.1038/s41598-018-23026-  
1538 w.  
1539 [39] C. Meagher, G. Arreaza, A. Peters, C.A. Strathdee, P.A. Gilbert, Q.-S. Mi, P. Santamaria, G.A. Dekaban, T.L.  
1540 Delovitch, CCL4 Protects From Type 1 Diabetes by Altering Islet β-Cell-Targeted Inflammatory Responses,  
1541 *Diabetes.* 56 (2007) 809–817. doi:10.2337/db06-0619.  
1542 [40] C.E.B. Couri, K.C.R. Malmegrim, M.C. Oliveira, New Horizons in the Treatment of Type 1 Diabetes: More  
1543 Intense Immunosuppression and Beta Cell Replacement, *Front. Immunol.* 9 (2018) 1086.  
1544 doi:10.3389/fimmu.2018.01086.  
1545 [41] F. Fagotto, R. Winklbauer, N. Rohani, Ephrin-Eph signaling in embryonic tissue separation, *Cell Adhes.*  
1546 *Migr.* 8 (2014) 308–326. doi:10.4161/19336918.2014.970028.  
1547 [42] A.W. Boyd, P.F. Bartlett, M. Lackmann, Therapeutic targeting of EPH receptors and their ligands, *Nat. Rev.*  
1548 *Drug Discov.* 13 (2014) 39–62. doi:10.1038/nrd4175.  
1549 [43] X.-T. Deng, M.-Z. Wu, N. Xu, P.-C. Ma, X.-J. Song, Activation of ephrinB-EphB receptor signalling in rat  
1550 spinal cord contributes to maintenance of diabetic neuropathic pain, *Eur. J. Pain Lond. Engl.* 21 (2017)  
1551 278–288. doi:10.1002/ejp.922.  
1552  
1553  
1554

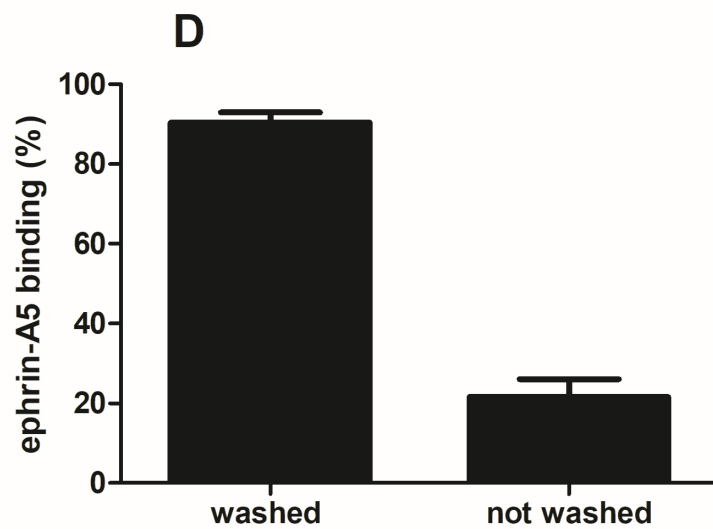
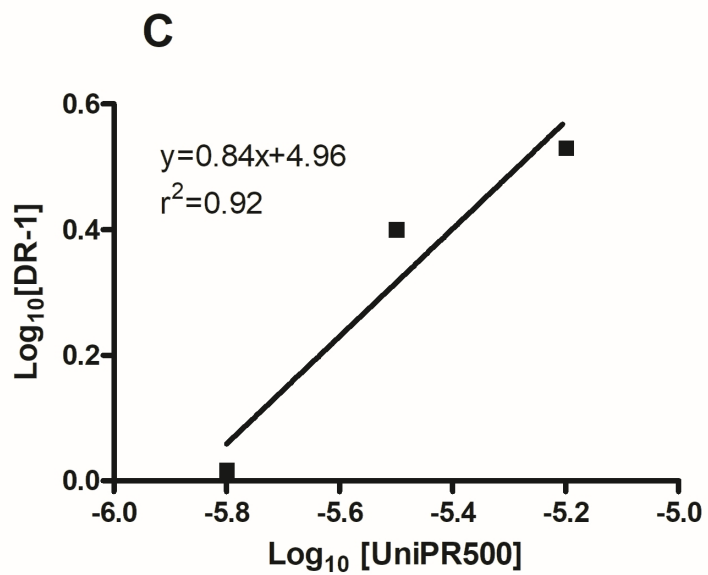
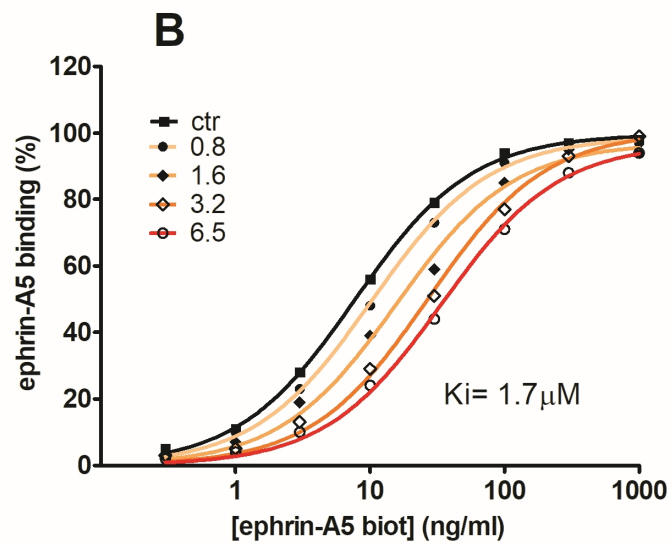
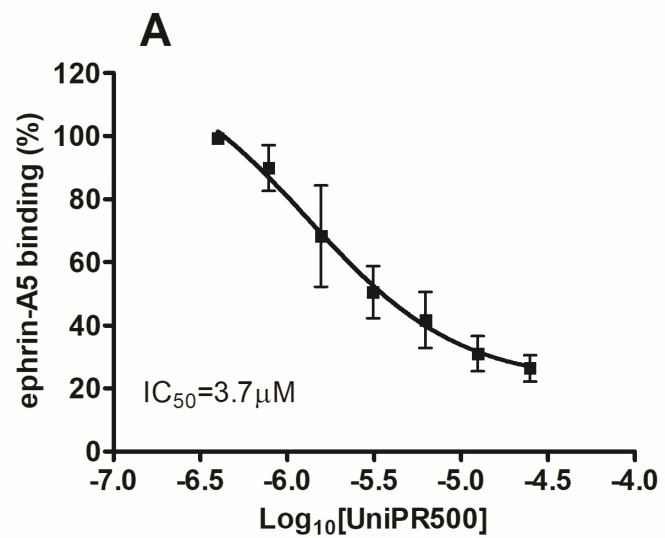
## 1555 CONFLICT OF INTEREST

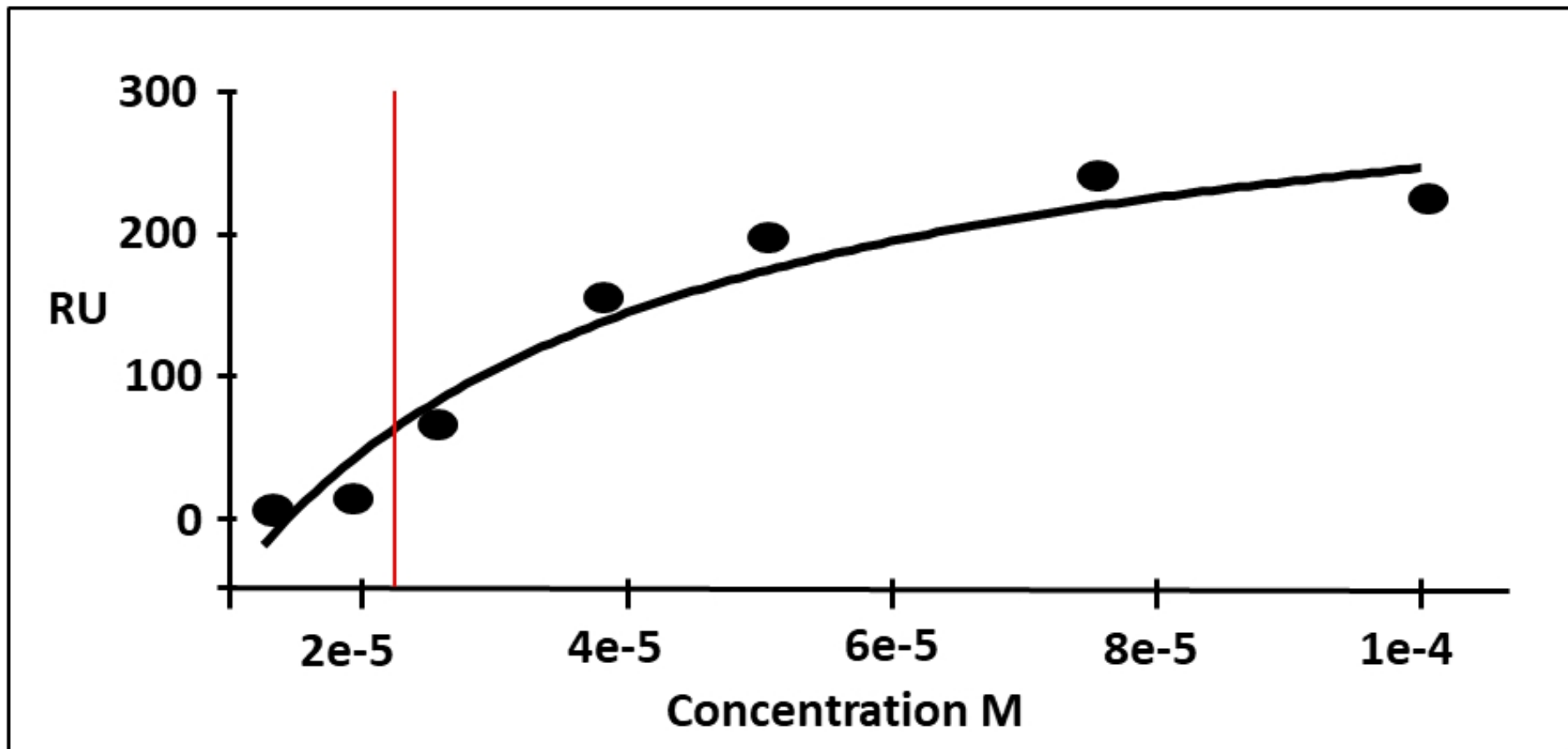
1556  
1557 The compound was patented by AL, MI and MT  
1558  
1559  
1560  
1561  
1562  
1563  
1564  
1565  
1566  
1567  
1568

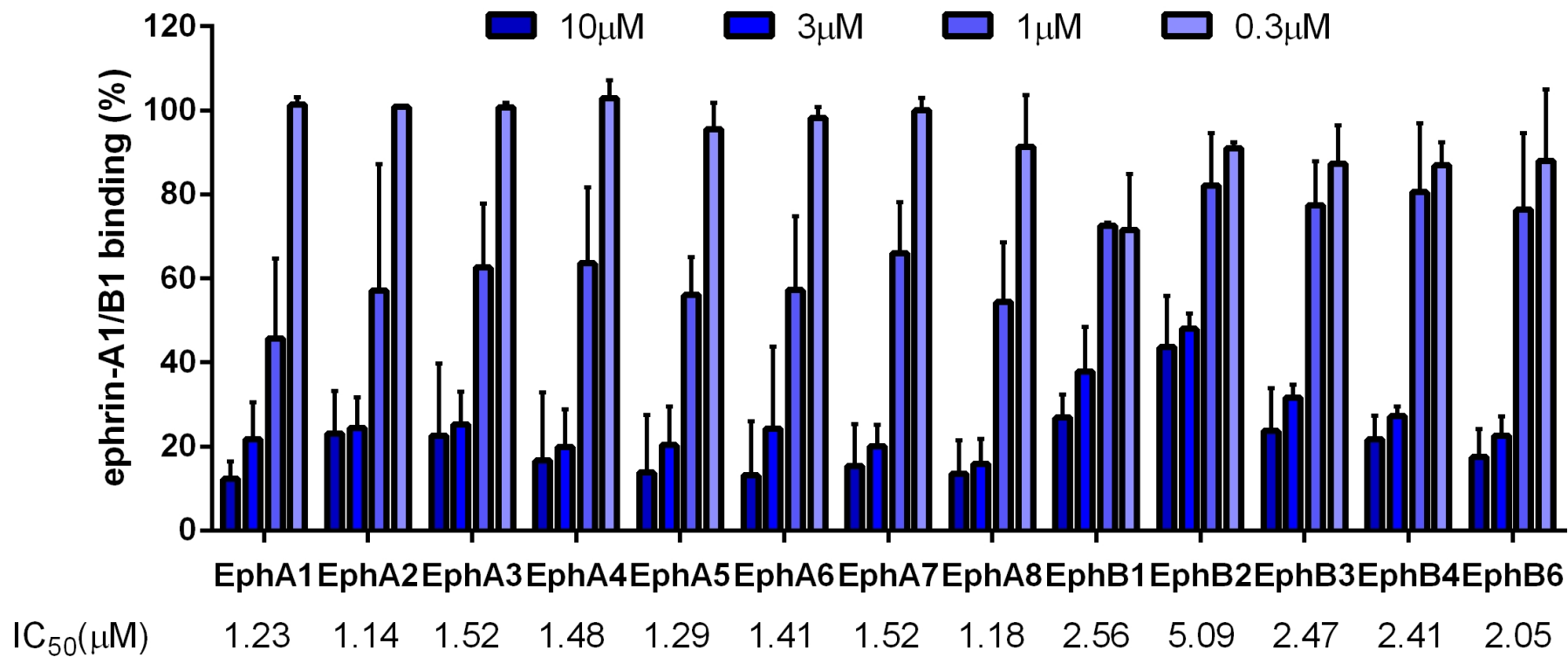


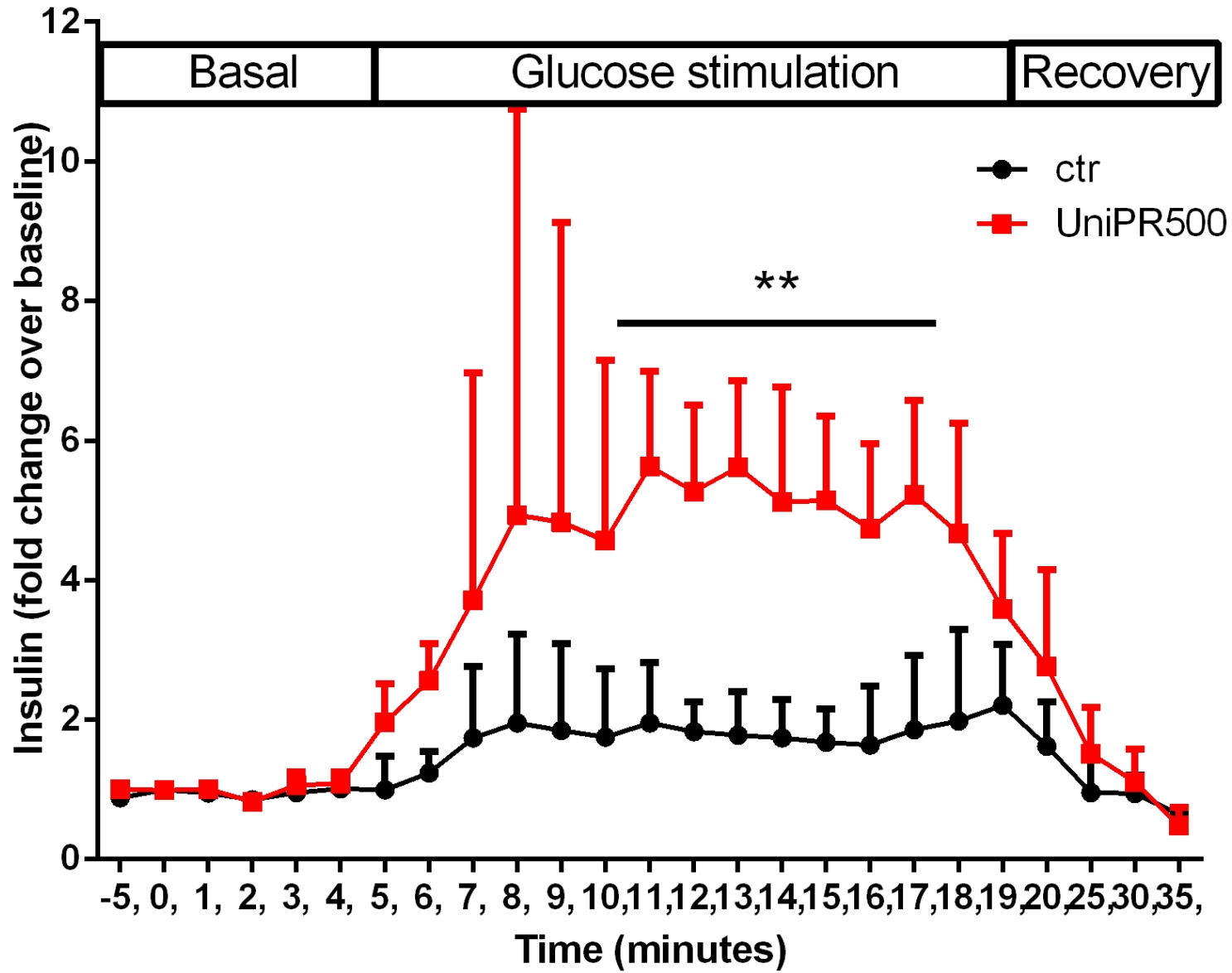
# TGR5

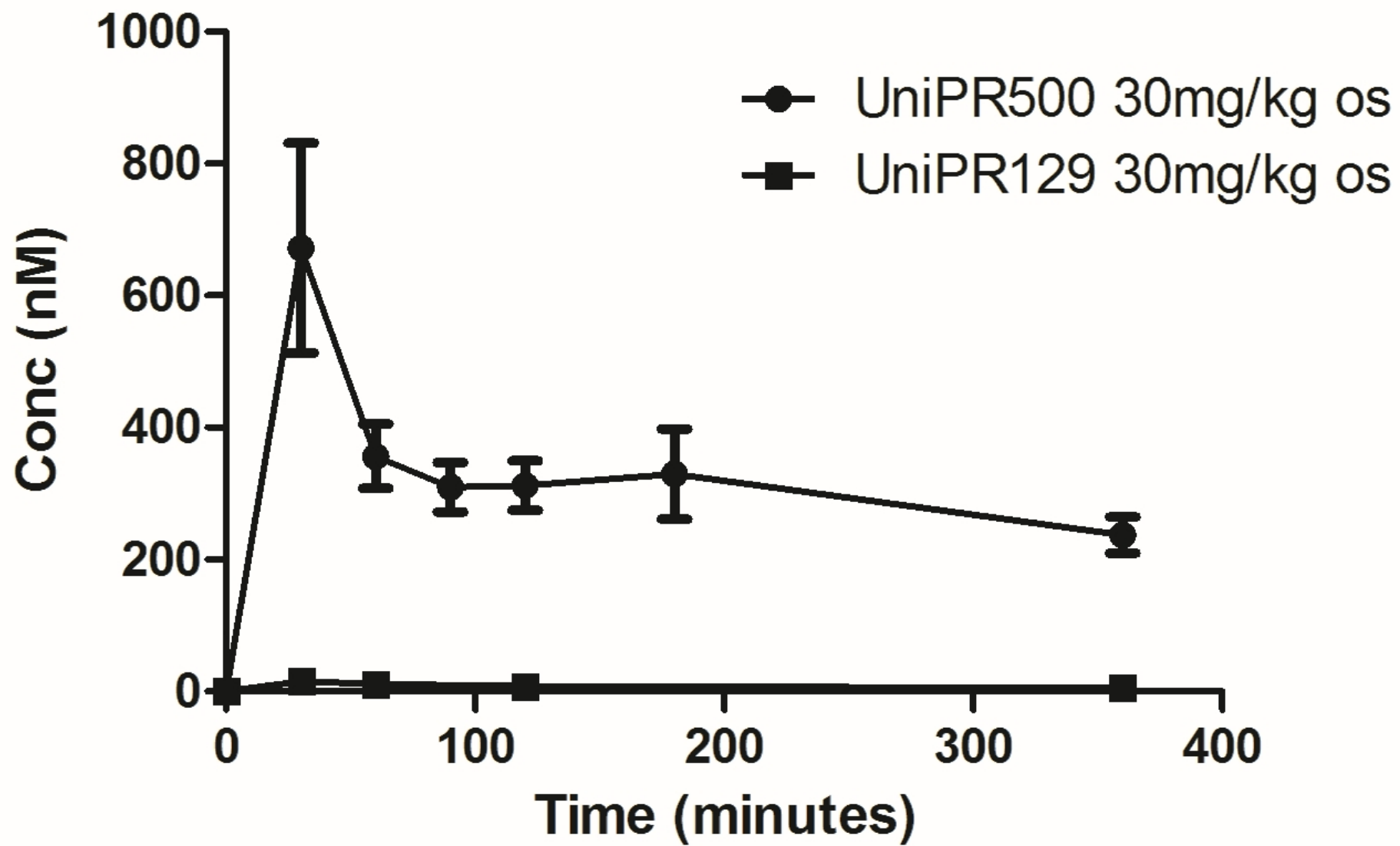


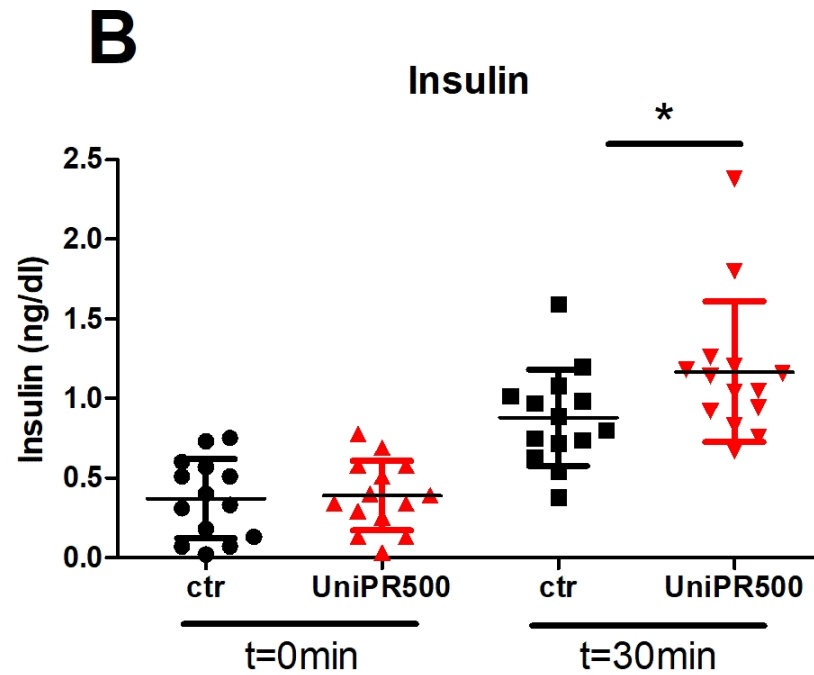
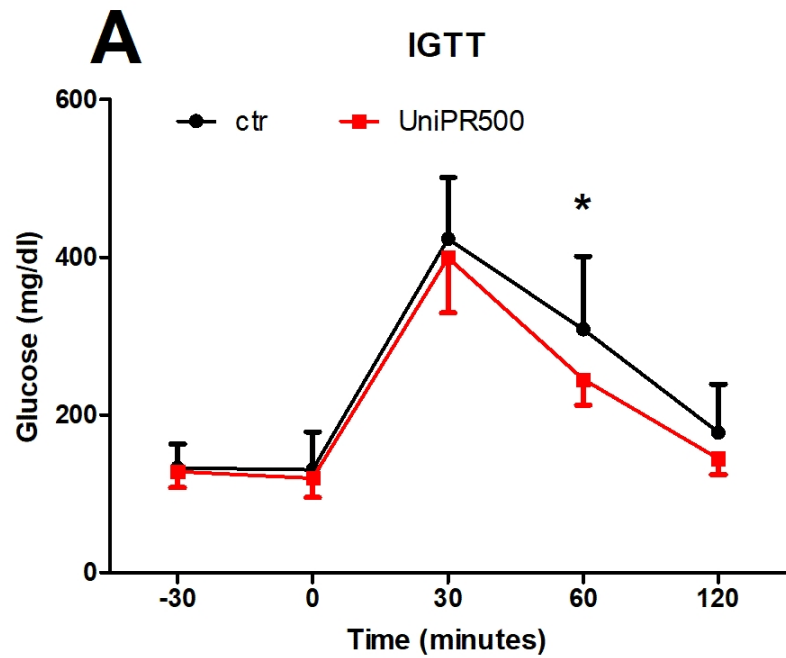


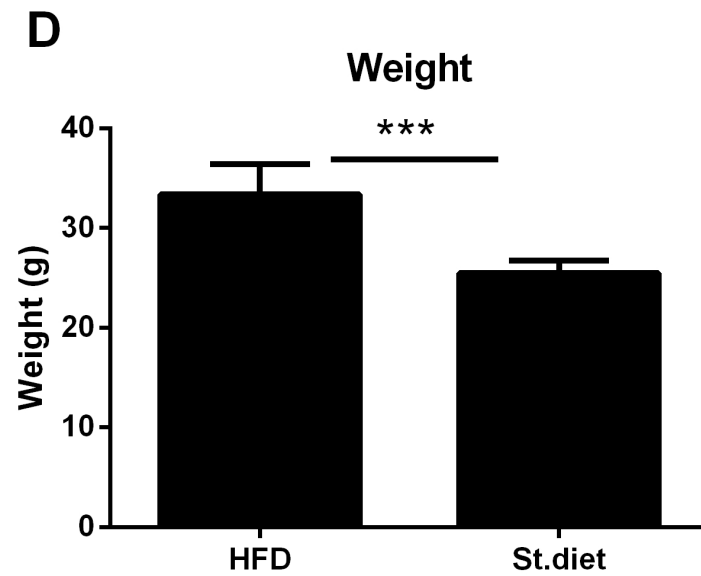
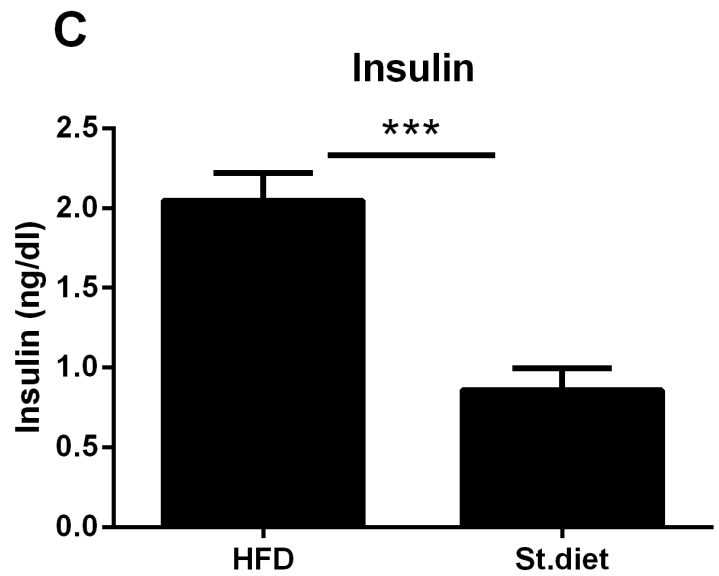
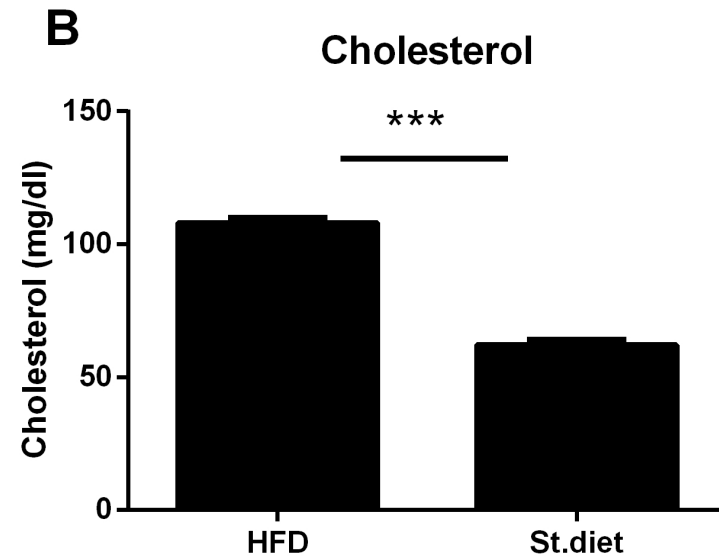
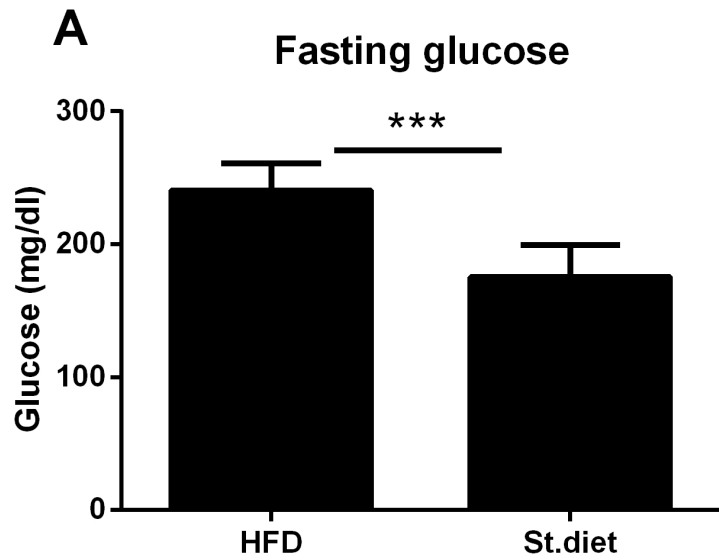


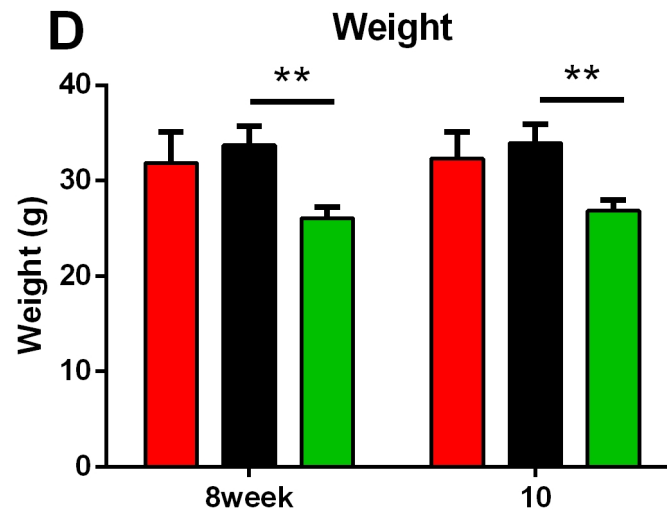
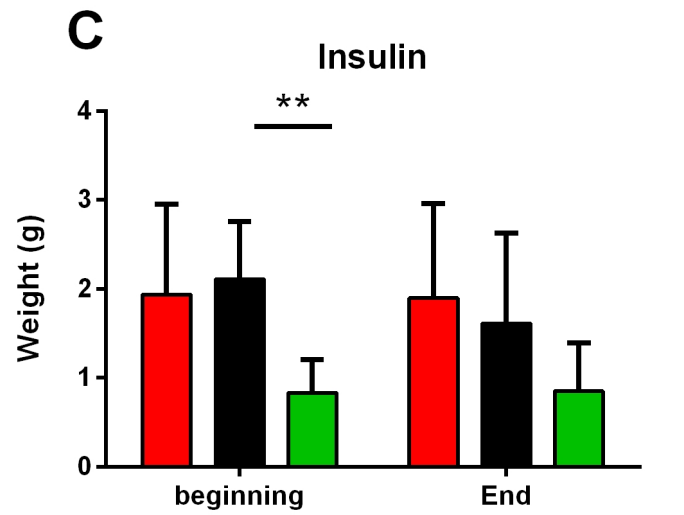
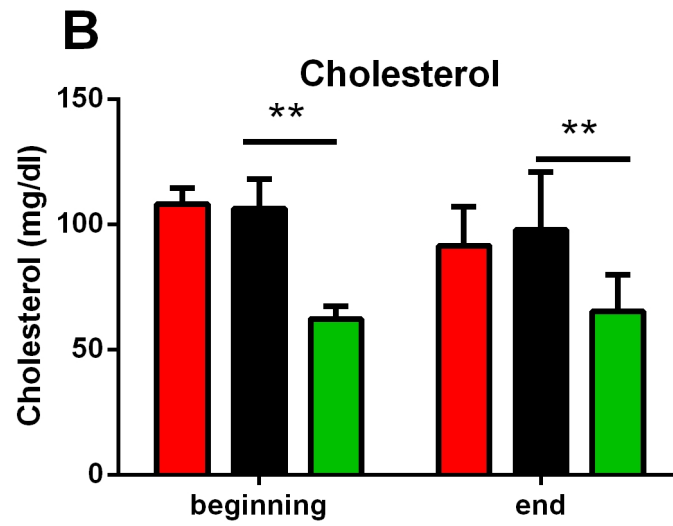
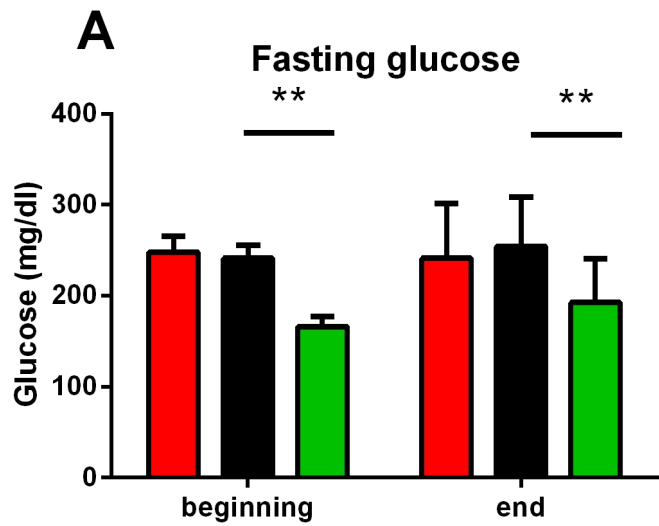






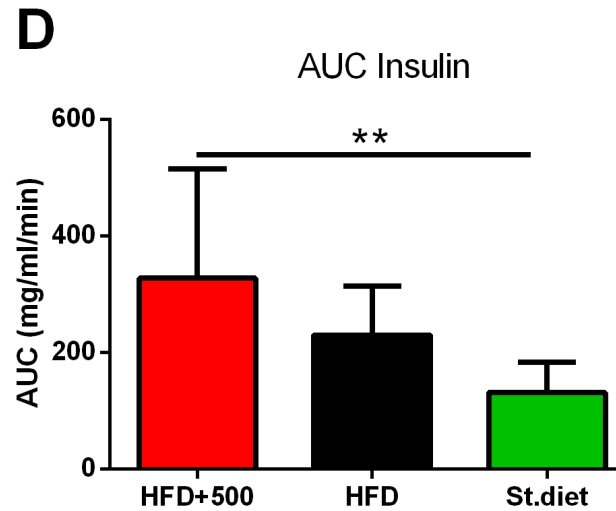
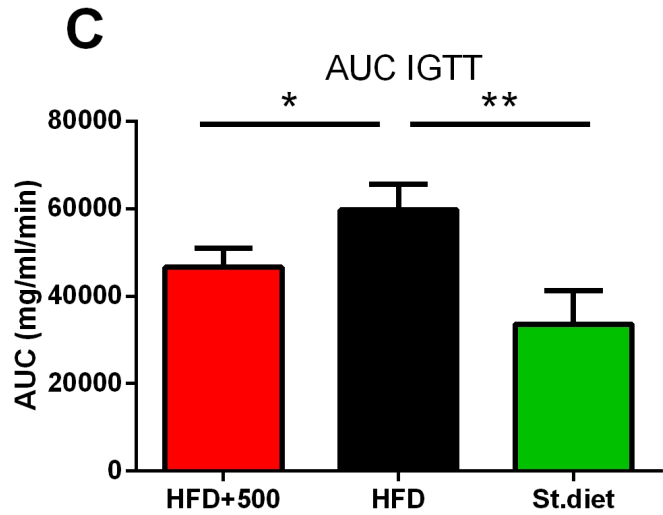
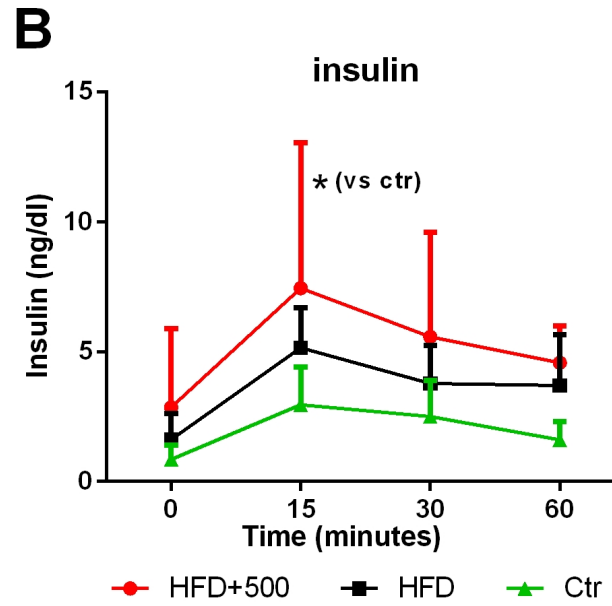
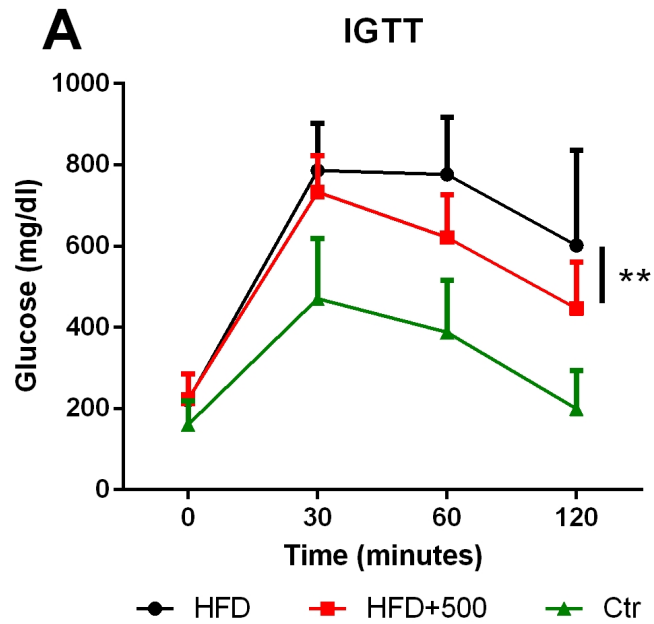


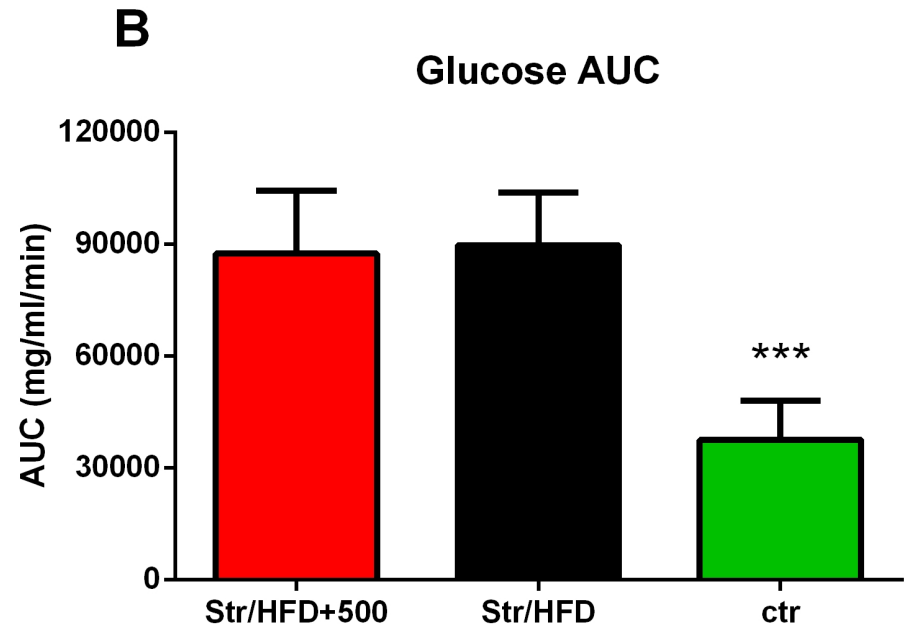
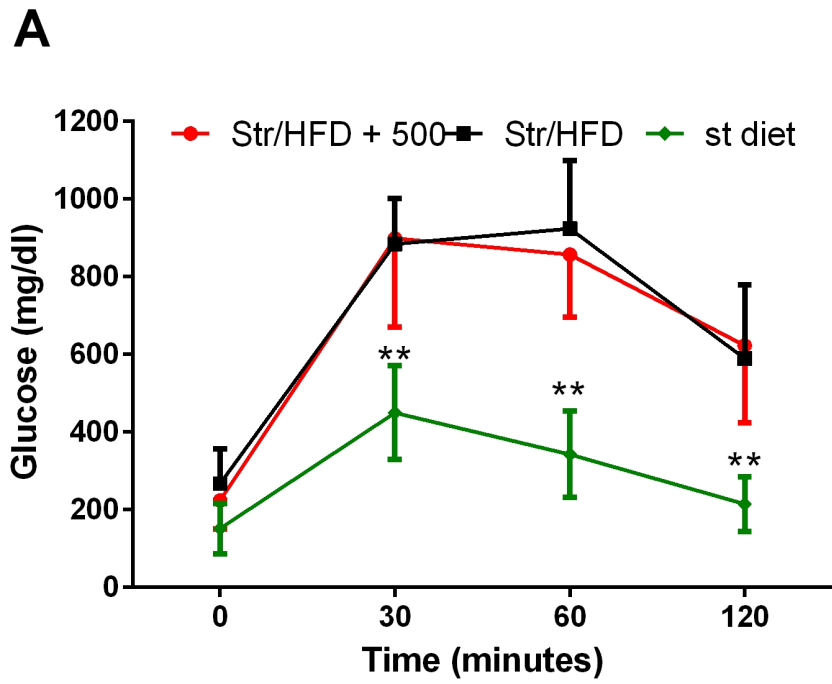




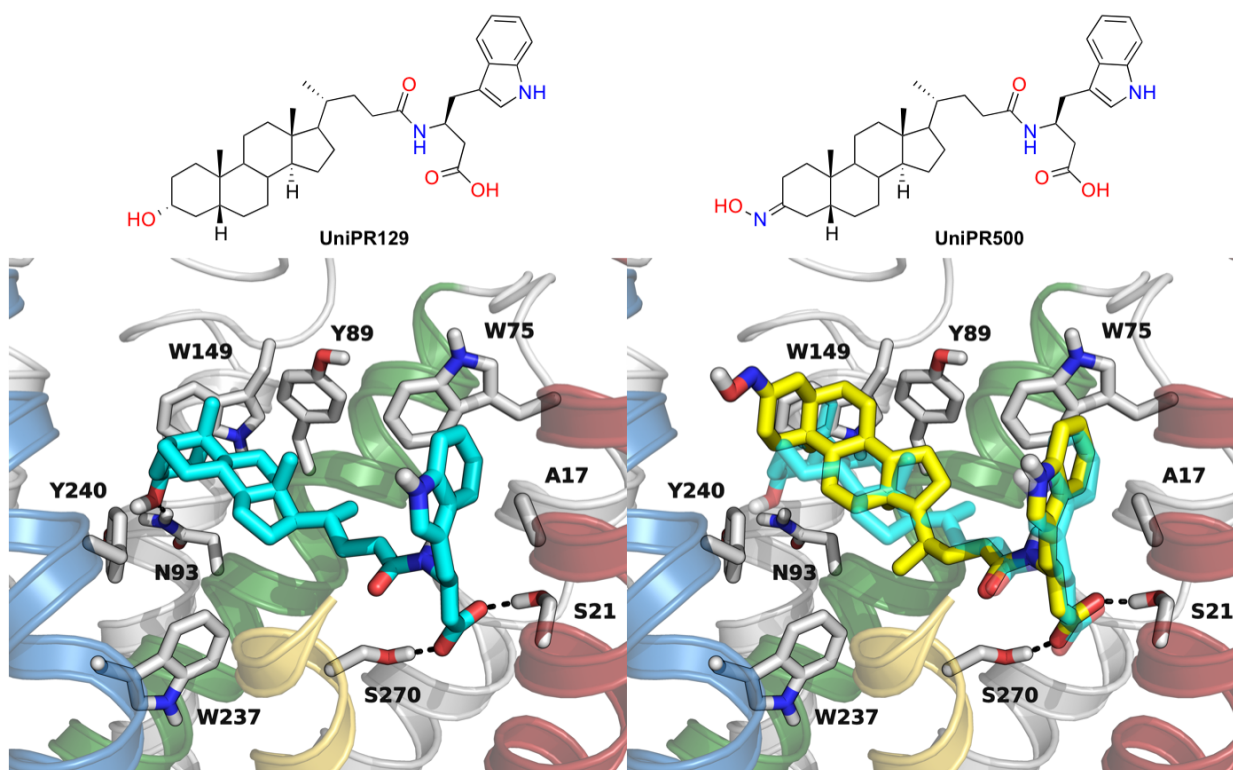
■ HFD+500 ■ HFD ■ St.diet

■ HFD+500 ■ HFD ■ St.diet



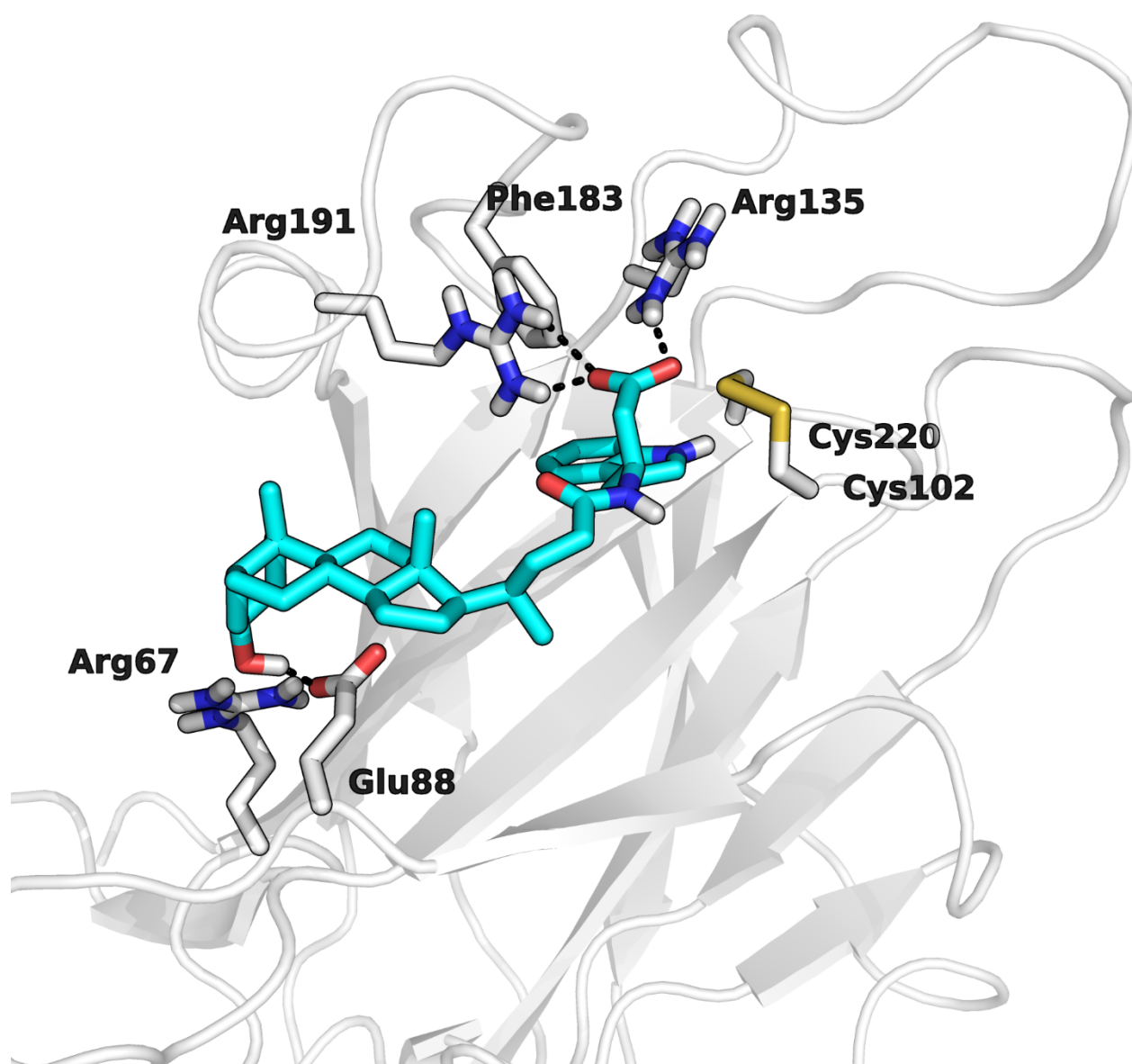


## Supplementary material 1

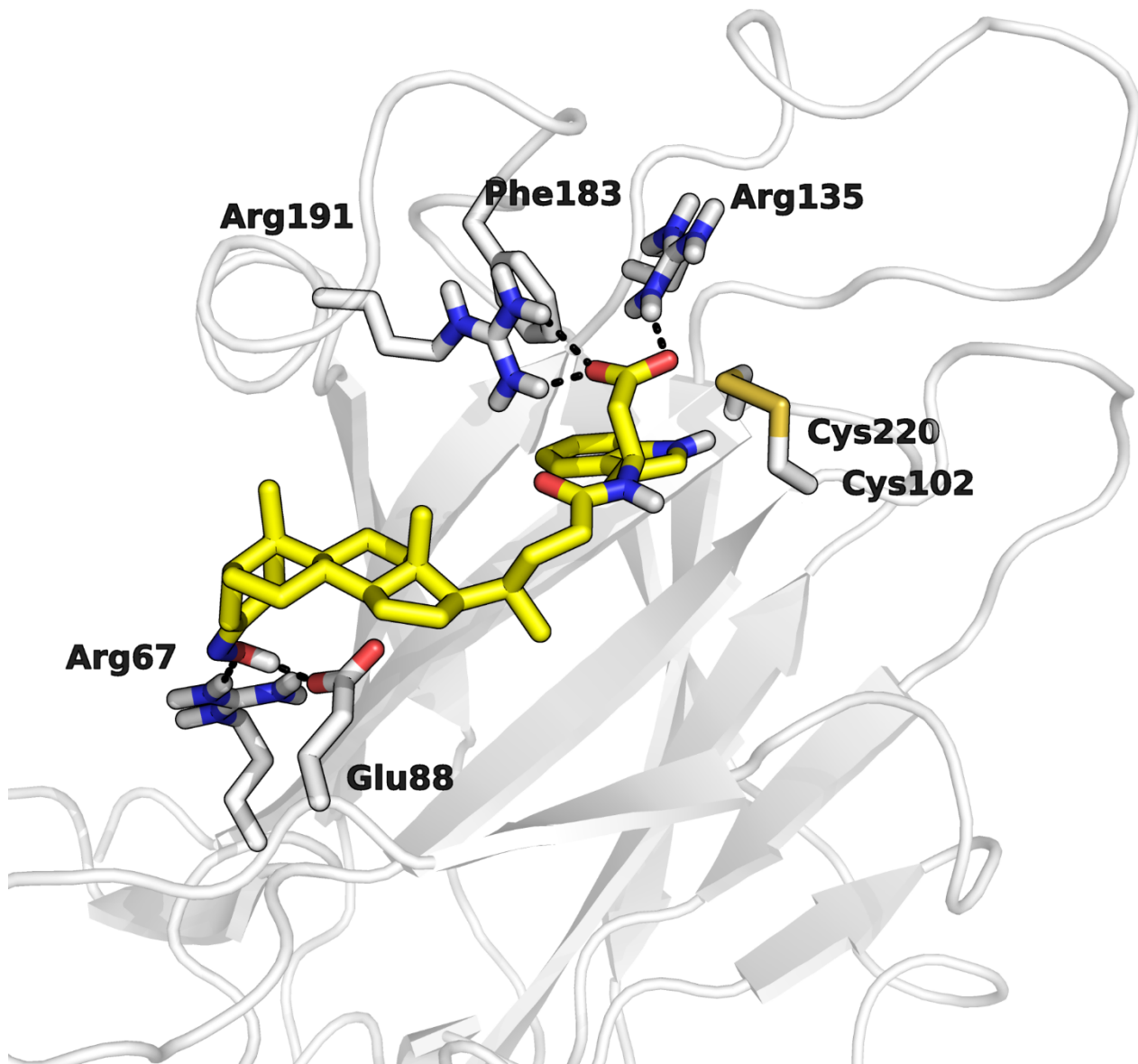


Binding mode of UniPR129 (left, cyan carbon atoms) and of UniPR500 (right, yellow carbon atoms) to TGR5 receptor (white carbon atoms).

Supplementary material 2



*Binding pose of UniPR129 (cyan carbon atoms) on EphA5 binding site (white carbon atoms). The overall structure of EphA5 is represented with white ribbons. EphA5 structure was taken from PDB (4ET7.pdb)*



*Binding pose of UniPR500 (yellow carbon atoms) on EphA5 binding site (white carbon atoms). The overall structure of EphA5 is represented with white ribbons. EphA5 structure was taken from PDB (4ET7.pdb)*

### Supplementary material 3

Anatomo-pathological analysis were performed on streptozotocin-HFD mice treated and untreated with UniPR500 30mg/kg os for 14 days as described in the main text. Liver, kidneys, pancreas were collected from each mice and samples were immediately fixed in 10% neutral buffered formalin. After paraffin embedding, 4-5 µm thick sections were obtained with microtome (Leica), stained with Hematoxylin and Eosin (H&E) and Periodic acid-Schiff (PAS). Histological slides were examined with Nikon Eclipse E800 microscope (Nikon Corporation, Japan) using Nikon PLAN APO lenses. Sections were photographed at 4x, 10x, 20x and 40x (Nikon PLAN APO lenses) with Camera DIGITAL SIGHT DS-Fi1 (Nikon Corporation, made in Japan); pictures were acquired with DS Camera Control Unit DS-L2 (Nikon Corporation, Japan) and stored in USB device. Histological lesions were graded and classified based on the extension/distribution (focal, multifocal and diffuse) and severity (scant, mild, moderate, severe).

#### Results:

No gross lesions were detected in treated or untreated mice during necroscopy.

#### **Mice 1-2-3-4-14 (streptozotocin-HFD mice treated with UniPR500 for 14 days)**

- Pancreas: In diabetic mice treated for 15 days with UNIPR500, inflammatory or regressive injuries were not observed on the exocrine pancreas; the islets were rare, both small or large, frequently adjacent to small vascular or ductular structures: numerous pancreatic islets cells presented a cytoplasmatic vacuolation (3/5) or perinsular lymphocytic infiltration (insulitis) (2/5)
- Liver: The liver parenchyma showed multifocal micro and macrovesicular steatosis, that affected one or more hepatic lobes, in all the examined mice (5/5), with scant interstitial or periportal lymphocytic infiltrates.
- Kidney: In all the diabetic treated mice no regressive injuries were observed on the tubular epithelial cells; scant perivascular lymphocytic infiltrates were present in 3 mice (3/5). With the PAS stain, slight thickening of Bowman's capsule were highlighted in all examined mice (5/5)

#### **Mice 6-8-9-10-12 (streptozotocin-HFD mice untreated with UniPR500)**

- Pancreas; pancreatic islets were small or large, frequently adjacent to vascular or ductular structures. In 2 untreated mice (2/5) islet cells showed morphological alterations with a large nucleus or cytoplasm vacuolation; in one mouse (1/5) perinsular lymphocytic infiltration were observed; another mouse showed focal necrosis of acinar cells with mild neutrophilic infiltration.
- Liver; focal or multifocal micro/macrovesicular steatosis were observed in all streptozotocin-HFD untreated mice.
- Kidneys: In all the mice no regressive injures affecting the tubular epithelial cells; 3/5 mice present scant or mild perivascular infiltrates of lymphocytes. With PAS stain, slight thickening of Bowman's capsule were highlighted in all mice.

Accordingly to the histopathological features, no significant differences have been showed between the streptozotocin-HFD mice treated with UNIPR500 and streptozotocin-HFD untreated mice; both groups showed endocrine pancreatic injuries, islet cells vacuolation and lymphocytes infiltration, indicative of IDDM, mild or severe degenerative changes (steatosis) in the liver, slight focal interstitial inflammation in kidneys.

## Pancreas

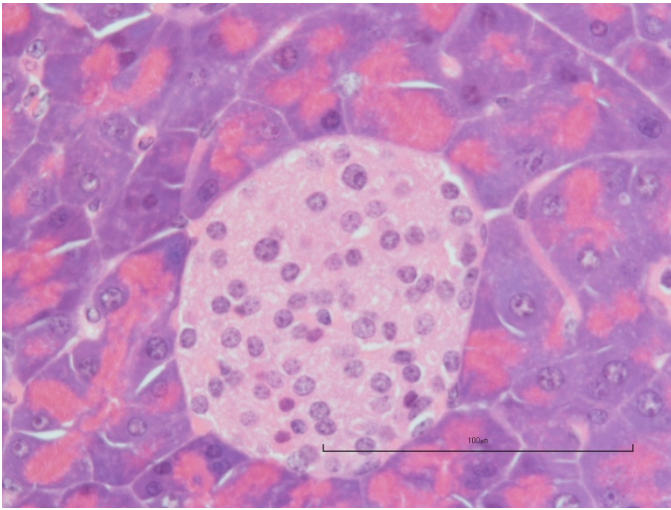


Fig.1-Pancreas of control mouse with normal pancreatic islet (H-E, 40x)

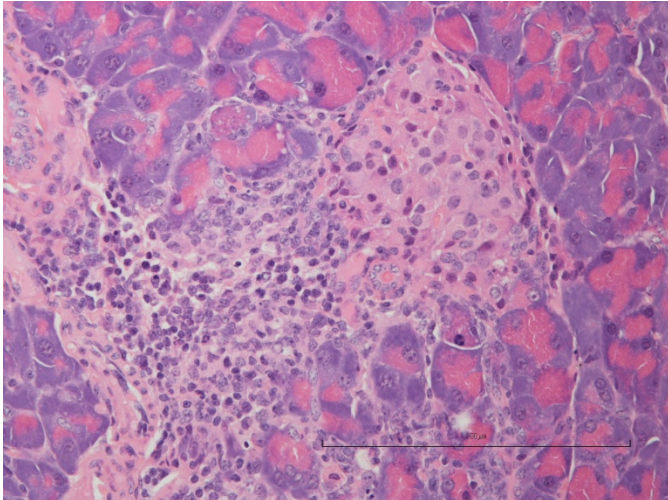


Fig 2 Pancreas- Streptozocin-HFD untreated mouse: peri-insular severe lymphocytic infiltration (insulitis) (H-E, 40x)

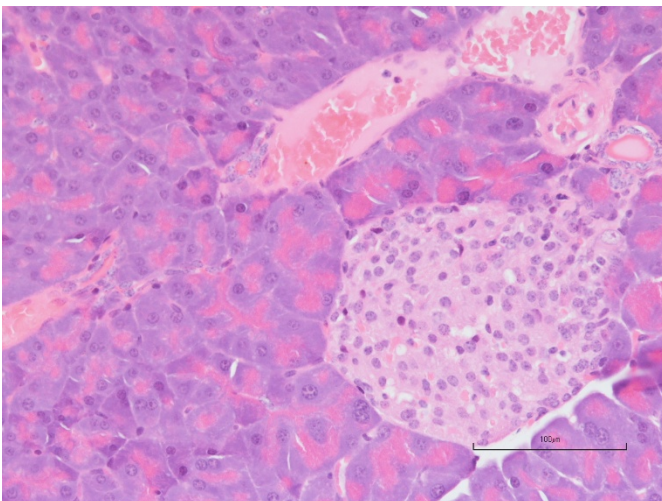


Fig.3- Pancreas- Streptozocin-HFD mouse treated with UniPR500: mild cytoplasmic vacuolation of pancreatic islets (H-E, 20x)

## Kidney

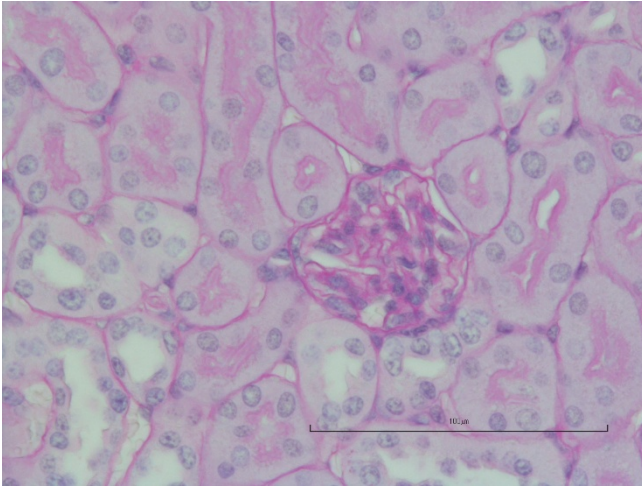


Fig.4: Kidney of control mouse showing the normal histological structure of renal parenchyma, (PAS stain, 40x)

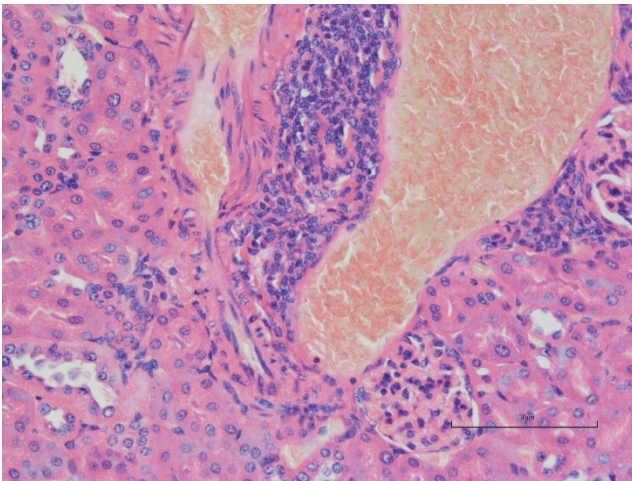


Fig 5-Kidneys-Perivascular infiltrates of lymphocytes in Streptozocin-HFD untreated mice (H-E stain-20x)

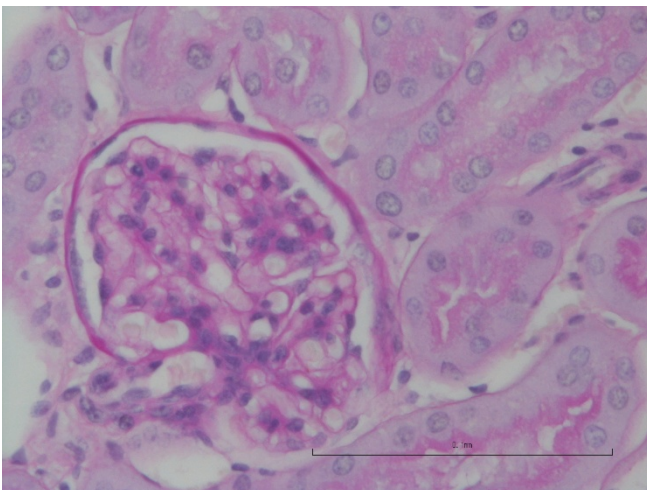


Fig 6 -Kidney- Slight thickening of Bowman's capsule were highlighted in Streptozocin-HFD treated mice with UniPR500 (PAS stain -40x)

## Liver

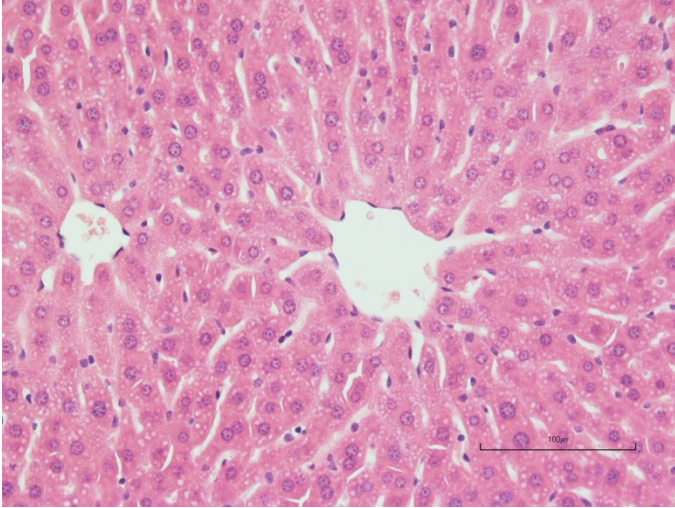


Fig 7- Liver of control mouse with normal hepatocytes (H-E, 20x)

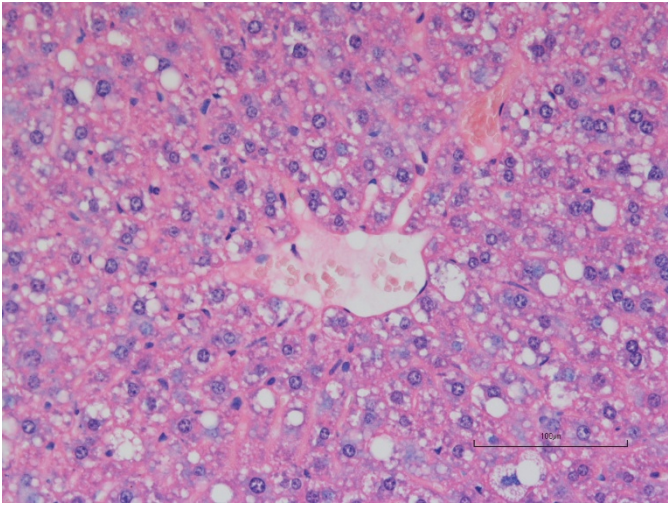


Fig. 8 Liver- Streptozocin-HFD untreated mice showed severe steatosis (H-E, 20X)

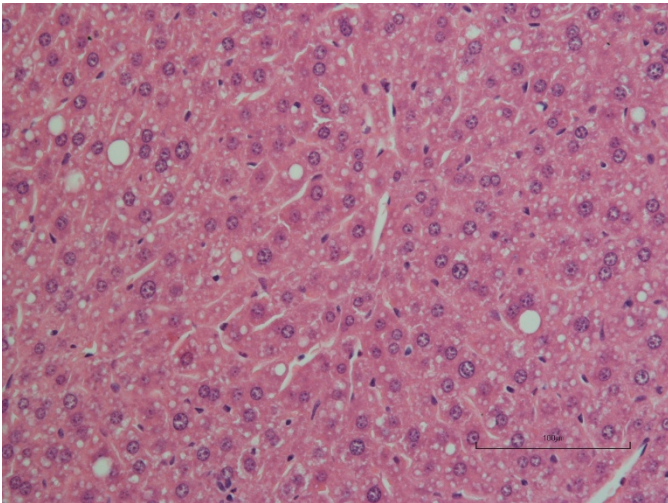


Fig 9 - Liver- Streptozocin-HFD treated mice with UniPR500 showed mild steatosis (H-E, 20X)

Table 1. Selectivity panel for the Eph-ephrin antagonist UniPR500. The compound was tested at single dose (10  $\mu$ M) in triplicate. The biological activity of a reference standard for each target is also reported.

Target	test	%inhibition or activation ( $\pm$ SD)	Standard IC <sub>50</sub> or EC <sub>50</sub>
GLP1, agonism 2181	Cellular functional assay GPCR/cAMP/HTRF	0.4 $\pm$ 0.2	GLP-1 (7-37), 0.052nM
GLP1, antagonism 2182	Cellular functional assay GPCR/cAMP/HTRF	13 $\pm$ 12	exendin-3(9-39), 5.7nM
PPAR- $\gamma$ , agonism 2771	Nuclear functional assay Coactivator recruitment/alphascreen	0.0 $\pm$ 0.0	Rosiglitazone, 190nM
PPAR- $\gamma$ , antagonism 2772	Nuclear functional assay Coactivator recruitment/alphascreen	-2.4 $\pm$ 6.8	GW9662, 91nM
PTP1B, inhibition 2593	Enzyme assay, fluorogenic substrate	-4.5 $\pm$ 0.7	(NH <sub>4</sub> ) <sub>6</sub> Mo <sub>7</sub> O <sub>24</sub> , 12nM
DPP IV, 2942	Enzyme assay, fluorogenic substrate	-3.3 $\pm$ 3.5	K579, 3nM
K <sub>ATP</sub> channel, 0165	Radioligand assay	7.0 $\pm$ 9.8	Glibenclamide, 0.25nM

Table 2. Physicochemical properties, ASBT binding and *in vitro* stability of UniPR500

Cpd	$\log D_{\text{Oct},7.4}$	solubility <sup>a</sup> ( $\mu\text{M}$ )	% ASBT binding <sup>b</sup>	% remaining compound in plasma <sup>c</sup>	% remaining compound in liver <sup>d</sup>
<b>UniPR129</b>	$4.90 \pm 0.15^e$	$31.8 \pm 4.2^e$	$22.7 \pm 2.4$	$98.3 \pm 9.5^e$	$56 \pm 5^e$
<b>UniPR500</b>	$4.23 \pm 0.11^e$	$51.9 \pm 4.4^e$	$92.6 \pm 1.5$	$93.7 \pm 11.3^e$	$70 \pm 7^e$

<sup>a</sup>From DMSO stock solution. <sup>b</sup>Percent bound at 10  $\mu\text{M}$  <sup>c</sup>Percent remaining after 24h of incubation, 37 °C <sup>d</sup>Percent remaining after 1 h incubation in the presence of a NADPH-regenerating system in liver S9 fraction <sup>e</sup> data from (Incerti et al., 2017). Data are the means of at least three independent experiments  $\pm$  SEM.

M. Tognolini, A. Lodola and M. Incerti patented the described compound (Italian patent 0001426534, no extensions).